

NACA RM SE54K19

Restriction/Classification Cancelled

CONFIDENTIAL  
CLASSIFICATION CANCELLED  
Authority: NACA, Title 18, U.S.C.  
ANNOUNCEMENTS BY  
Date: 2/25/70

PERMANENT FILE COPY

# RESEARCH MEMORANDUM

for the

Bureau of Aeronautics, Department of the Navy

PRELIMINARY DATA ON THE EFFECTS OF INLET PRESSURE  
DISTORTIONS ON THE J57-P-1 TURBOJET ENGINE

By Lewis E. Wallner, Robert J. Lubick, and Thomas H. Einstein

Lewis Flight Propulsion Laboratory  
Cleveland, Ohio

Restriction/Classification Cancelled

This material contains information of the espionage laws, Title 18, in a manner to unauthorized person is prohibited.

United States within the meaning of the espionage laws, Title 18, in a manner to unauthorized person is prohibited.

## NATIONAL ADVISORY COMMITTEE FOR AERONAUTICS

WASHINGTON, D.C.

FILE COPY

To be referred to  
the National Technical Information Service  
for Aeronautics  
Washington, D.C.

CONFIDENTIAL  
CLASSIFICATION CANCELLED  
Authority: NACA, Title 18, U.S.C.  
ANNOUNCEMENTS BY  
Date: 2/25/70

16

12-808-54

NACA RM SE54K19

**CONFIDENTIAL**  
**CLASSIFICATION CANCELLED**  
Authority NASA PUBLICATIONS  
ANNOUNCEMENTS NO.  
Date \_\_\_\_\_ By \_\_\_\_\_

#### FOREWORD

To permit expeditious transmittal of performance data to those concerned, figures of "Preliminary Data" are presented herein. Preliminary Data are test data that have not received the complete analysis and extensive cross-checking normally given a set of NACA data before release.

**CONFIDENTIAL**  
**CLASSIFICATION CANCELLED**  
Authority NASA PUBLICATIONS  
ANNOUNCEMENTS NO.  
Date \_\_\_\_\_ By \_\_\_\_\_

## NATIONAL ADVISORY COMMITTEE FOR AERONAUTICS

RESEARCH MEMORANDUM

for the

Bureau of Aeronautics, Department of the Navy

PRELIMINARY DATA ON THE EFFECTS OF INLET PRESSURE DISTORTIONS  
ON THE J57-P-1 TURBOJET ENGINE

By Lewis E. Wallner, Robert J. Lubick, and Thomas H. Einstein

## SUMMARY

An investigation to determine the steady-state and surge characteristics of the J57-P-1 two-spool turbojet engine with various inlet air-flow distortions was conducted in the altitude wind tunnel at the NACA Lewis laboratory. Along with a uniform inlet total-pressure distribution, one circumferential and three radial pressure distortions were investigated. Data were obtained over a complete range of compressor speeds both with and without intercompressor air bleed at a flight Mach number of 0.8 and at altitudes of 35,000 and 50,000 feet.

Total-pressure distortions of the magnitudes investigated had very little effect on the steady-state operating line for either the outer or inner compressor. The small radial distortions investigated also had little if any effect on narrowing the high speed operating range of the engine over that obtained with the uniform inlet pressure distribution. The circumferential distortion, however, raised the minimum speed at which the engine could operate without encountering surge when the intercompressor bleeds were closed. This increase in minimum speed resulted in a substantial reduction in the operable speed range accompanied by a reduction in the altitude operating limit.

## INTRODUCTION

At the request of the Navy Department, Bureau of Aeronautics, an investigation was conducted to determine the steady-state and transient performance of the J57-P-1 turbojet engine in the altitude wind tunnel at the NACA Lewis laboratory. As part of this investigation, the steady-state operating line and the operating condition of the two compressors at the point where the engine surged were determined. These data are reported herein for a uniform inlet total-pressure distribution, for one circumferential inlet pressure distortion, and for three relatively small radial pressure distortions.

Data were obtained over a complete range of rotor speeds at altitudes of 35,000 and 50,000 feet and at a flight Mach number of 0.8. At each flight condition, the steady-state operating line and the operating line when engine surge occurs were determined for both compressors with and without compressor air bleed.

## ENGINE INSTALLATION AND INSTRUMENTATION

### Engine and Installation

A cross-sectional view of the J57-P-1 two-spool turbojet engine is shown in figure 1. The inner spool consists of a 7-stage axial-flow compressor connected by a hollow shaft to a single-stage shrouded turbine. The outer spool consists of a 9-stage axial-flow compressor and a 2-stage shrouded turbine connected by a shaft inside of and concentric with the hollow shaft of the inner spool. Rated inner spool speed is approximately 9600 rpm. The combustor is of the cannular type having eight tubular liners each with a piloting cone and six duplex fuel spray nozzles.

The engine is equipped with two compressor bleed ports that permit the bleeding of air from the discharge of the outer compressor, thereby lowering the outer compressor pressure ratio to avoid outer compressor surge. Opening and closing of the compressor bleeds is controlled by the outer-spool speed. The outer-spool speed at which the bleeds are actuated is scheduled as a function of inlet temperature with the actual speed ~~decreasing~~ <sup>INCREASING</sup> with increasing inlet temperature. This schedule is such that the bleeds operate from one position to the other between outer-spool speeds of 5195 and 5660 rpm.

The turbojet engine was mounted on a wing section that spanned the test section of the altitude wind tunnel. Ambient air was dried and refrigerated and then supplied to the engine by means of inlet ducting. Automatic bleed valves in the inlet ducting were used to maintain the ram-pressure ratio at the desired level during transient engine operation.

### Instrumentation

Instrumentation used to measure the steady-state compressor performance is indicated in figure 1. The following parameters were measured on a multiple-channel oscillograph both during steady-state and transient operation: (1) outer and inner compressor speed; (2) inlet and outlet pressures for both outer and inner compressor; (3) inner compressor inlet temperature. The presence of rotating stall was indicated by oscilloscope observations of compressor inner-stage pressure pickups and hot-wire anemometer signals.

## Types of Inlet Pressure Distortions

The inlet pressure distortions were produced by screen segments installed at the engine inlet 13 inches upstream of the inlet guide vanes (fig. 2). In order to support the fine mesh screens, a  $\frac{1}{4}$ -inch mesh screen was placed over the entire annulus. The uniform inlet total-pressure distribution is therefore the profile existing behind this screen.

The configurations and sizes of the screens are described in the following table and their location schematically shown in figure 3.

Configuration	Type of distortion	Size of screen	Size of backing screen
Undistorted	Uniform	None	$\frac{1}{4}$ -inch mesh
A	Circumferential	0-#10-#20-#30 mesh	$\frac{1}{4}$ -inch mesh
B	Mild Radial	0-#7-#10 mesh	$\frac{1}{4}$ -inch mesh
C	Severe Radial	0-#10-#16 mesh	$\frac{1}{4}$ -inch mesh
D	Inverse Radial	#10-#7-0 mesh	$\frac{1}{4}$ -inch mesh

## PROCEDURE

Data were obtained at a flight Mach number of 0.80 at altitudes of 35,000 and 50,000 feet for the uniform inlet air-flow distribution, the circumferential air-flow distortion, and the three radial air-flow distortions. The surge characteristics were determined over the complete range of spool speeds with the restriction at the high-speed end being limiting turbine inlet temperature. The compressor bleeds were manually operated for this investigation so that the bleed valves could be held in either the open or closed position, independent of the normal bleed schedule.

For each engine inlet configuration, the steady-state operating line and engine surge line were determined for the engine with rated exhaust nozzle area. The operating conditions of the compressors at the point where the engine surged were obtained by using either step or ramp changes in fuel flow and recording the performance parameters on the transient instrumentation. The step and ramp changes in fuel flow were made possible by replacing the standard engine fuel control with a special fuel control.

The steady-state engine speed operational limits were determined by either slowly increasing or decreasing the speed at a constant flight condition until surge or limiting turbine temperature was encountered. In order to insure reliability in the data, each limit was based on from one to five data points, depending on the severity of the condition.

## RESULTS

The performance data are arranged in the figures according to the order presented in table I. The data as presented herein is merely the pressure ratio of each compressor at the point where engine surge occurred and not necessarily the surge pressure ratio of each compressor. Additional analysis and study are required before it can be determined which compressor surged initially at each engine surge point.

The shape and magnitude of the total-pressure distortions imposed on the engine at the inlet are presented in figures 4 and 5. It should be noted that the maximum radial distortion (fig. 5(a)) has local pressure deviations of only 2 or 3 percent in the tip region and about 7 percent in the hub region. The effect of these distortions on the speed match between the two spools, steady-state compressor operating lines, and compressor operating condition where engine surge occurred are shown in figures 6 to 10 for engine operation with intercompressor bleeds open at an altitude of 35,000 feet and a flight Mach number of 0.8. For the magnitude of distortions investigated, the speed match between the two spools (fig. 6) and the steady-state operating line for each compressor (figs. 7 and 8) remained essentially unaltered. This effect exists for both compressor bleed positions and both flight conditions investigated.

Figures 7 and 8 also compare the operating condition of the two compressors at the point where engine surge occurred for each configuration with the steady-state operating line for the same configuration. For the outer compressor, the pressure ratio at which the engine surged is approximately the same as the pressure ratio for steady state operation. This characteristic of the outer compressor existed for all engine and flight conditions investigated. The data of figure 7 and 8 are compared in figures 9 and 10 to show the effect of inlet pressure distortions on the point where engine surge occurs. In general, the inlet pressure distortions had little effect on the compressor pressure ratios with open bleeds at the engine surge condition.

For compressor bleeds closed at 35,000 feet (fig. 11 to 15) the small radial distortions had little effect on compressor operation. However, for the circumferential distortion, rotating stall was obtained over a somewhat enlarged speed range. At 50,000 feet with compressor bleeds open (figs. 16 to 20), the effects of inlet pressure distortions were relatively small; this is similar to the result at the lower altitude.

Rotating stalls persisted to higher engine speeds for all the inlet distortions with the compressor bleeds closed at 50,000 feet (fig. 21 to 25). High speed operation at this condition could not be obtained with the circumferential distortion because of steady state compressor surge.

The increase in inner-spool pressure ratio in the middle speed region with the circumferential distortion, shown in figures 15 and 20, is not necessarily an increase in surge pressure ratio of this compressor, but is simply the operating condition of this compressor at the moment of engine surge initiation.

The steady-state operating limits of the engine resulting from either maximum turbine-inlet temperature limit or the intersection of the steady-state operating line with the engine surge line are presented in figures 26 and 27. The shape of the limit lines for these data was determined from the data presented in reference 1. Figure 26 presents the limits with the intercompressor bleeds open. At this position of the bleeds no minimum speed limit was encountered; at 50,000 feet, high speed operation was limited by steady state engine surge for the undistorted inlet flow and inverse radial distortion, and by maximum exhaust gas temperature for the circumferential and radial distortion. As was demonstrated in reference 1, surge limited operation further reduces the maximum engine speed as altitude is increased above 50,000 feet.

Maximum speed operation for compressor bleeds closed (fig. 27) was not limited by engine surge, but only by encountering maximum exhaust gas temperature. Minimum speed operation was limited by steady-state surge; this speed limit was about the same for all configurations investigated except the circumferential distortion. At 35,000 feet, the circumferential distortion reduced the operable speed range by about 50 percent, whereas at 50,000 feet all operation with this distortion was precluded because of steady-state surge.

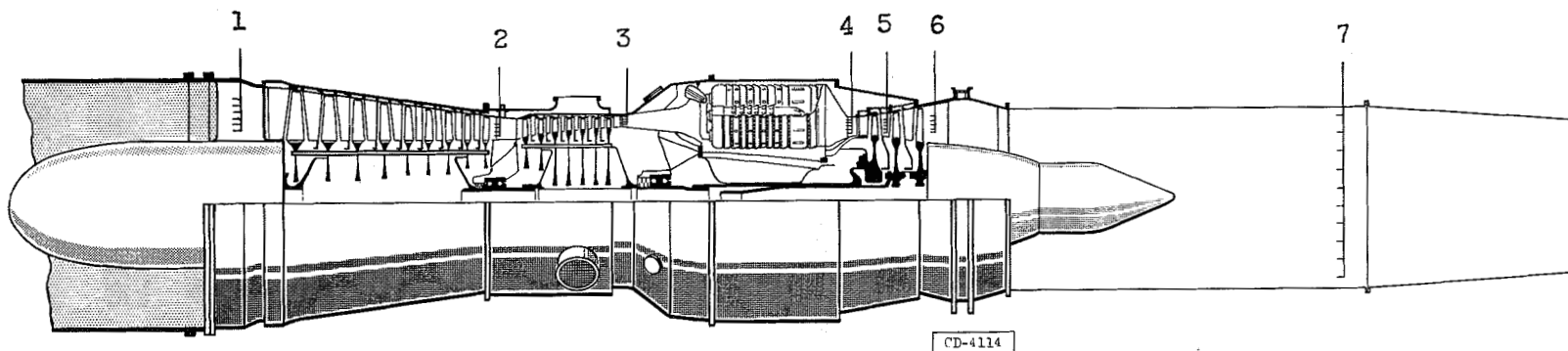
Lewis Flight Propulsion Laboratory  
National Advisory Committee for Aeronautics  
Cleveland, Ohio, December 3, 1954

#### REFERENCE

1. Wallner, Lewis E., and Saari, Martin J.: Preliminary Altitude Operational Characteristics of a J57-P-1 Turbojet Engine. NACA RM SE54C31, 1954.

TABLE I. - FIGURE INDEX

Figure	Dependent variable	Independent variable
1	Schematic diagram of engine	
2	Schematic diagram of engine inlet	
3	Schematic diagram of inlet screen configurations	
4(a)	Ratio of local total pressure average	Circumferential location
4(b)	Ratio of maximum pressure differential to average	$N_1/\sqrt{\theta_1}$
5(a)	Ratio of local total pressure to average.	Radial location
5(b)	Ratio of maximum pressure differential to average	$N_1/\sqrt{\theta_1}$
Bleeds open; altitude, 35,000 feet; flight Mach number 0.8		
6	$N_2/\sqrt{\theta_1}$ , $N_2/\sqrt{\theta_2}$	$N_1/\sqrt{\theta_1}$
7	$P_2/P_1$ } comparison of steady-state $P_3/P_2$ } and surge characteristics	$N_1/\sqrt{\theta_1}$
8		$N_2/\sqrt{\theta_2}$
9	$P_2/P_1$ } comparison of surge $P_3/P_2$ } characteristics	$N_1/\sqrt{\theta_1}$
10		$N_2/\sqrt{\theta_2}$
Bleeds closed; altitude, 35,000 feet; flight Mach number 0.8		
11	$N_2/\sqrt{\theta_1}$ , $N_2/\sqrt{\theta_2}$	$N_1/\sqrt{\theta_1}$
12	$P_2/P_1$ } comparison of steady-state $P_3/P_2$ } and surge characteristics	$N_1/\sqrt{\theta_1}$
13		$N_2/\sqrt{\theta_2}$
14	$P_2/P_1$ } comparison of surge $P_3/P_2$ } characteristics	$N_1/\sqrt{\theta_1}$
15		$N_2/\sqrt{\theta_2}$
Bleeds open; altitude, 50,000 feet; flight Mach number 0.8		
16	$N_2/\sqrt{\theta_1}$ , $N_2/\sqrt{\theta_2}$	$N_1/\sqrt{\theta_1}$
17	$P_2/P_1$ } comparison of steady-state $P_3/P_2$ } and surge characteristics	$N_1/\sqrt{\theta_1}$
18		$N_2/\sqrt{\theta_2}$
19	$P_2/P_1$ } comparison of surge $P_3/P_2$ } characteristics	$N_1/\sqrt{\theta_1}$
20		$N_2/\sqrt{\theta_2}$
Bleeds closed; altitude, 50,000 feet, flight Mach number 0.8		
21	$N_2/\sqrt{\theta_1}$ , $N_2/\sqrt{\theta_2}$	$N_1/\sqrt{\theta_1}$
22	$P_2/P_1$ } comparison of steady-state $P_3/P_2$ } and surge characteristics	$N_1/\sqrt{\theta_1}$
23		$N_2/\sqrt{\theta_2}$
24	$P_2/P_1$ } comparison of surge $P_3/P_2$ } characteristics	$N_1/\sqrt{\theta_1}$
25		$N_2/\sqrt{\theta_2}$
Steady-state operational limits		
26	Altitude (bleeds open)	$N_1/\sqrt{\theta_1}$
27	Altitude (bleeds closed)	$N_1/\sqrt{\theta_1}$



Station	Number of total pressure probes	Number of static pressure probes	Number of thermocouple probes
1	42	16	16
2	24	-	12
3	20	-	12
4	18	-	8
5	16	-	-
6	24	8	24
7	24	4	24

Figure 1. - Schematic diagram of J57-P-1 turbojet engine showing location and amount of steady-state instrumentation.

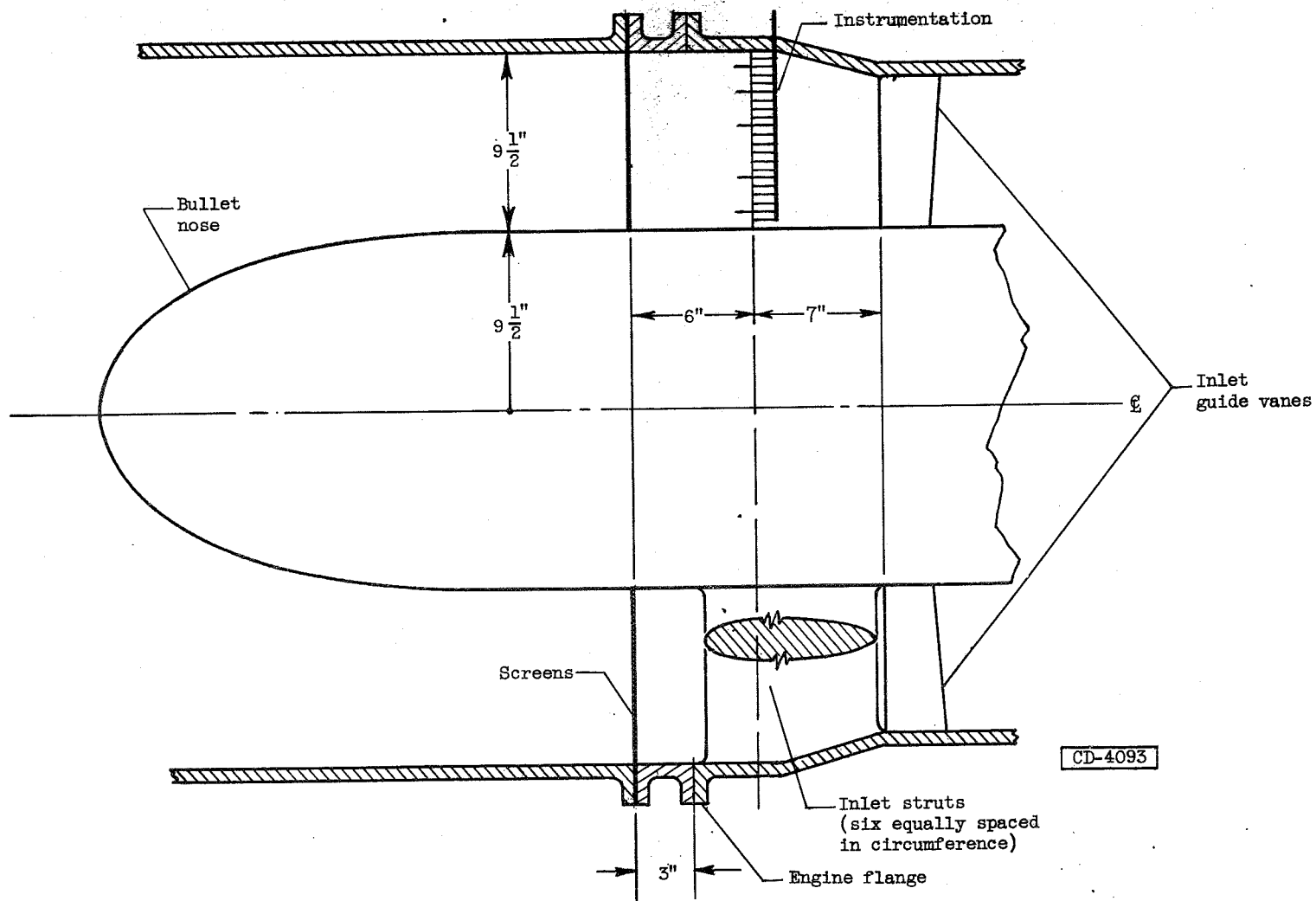
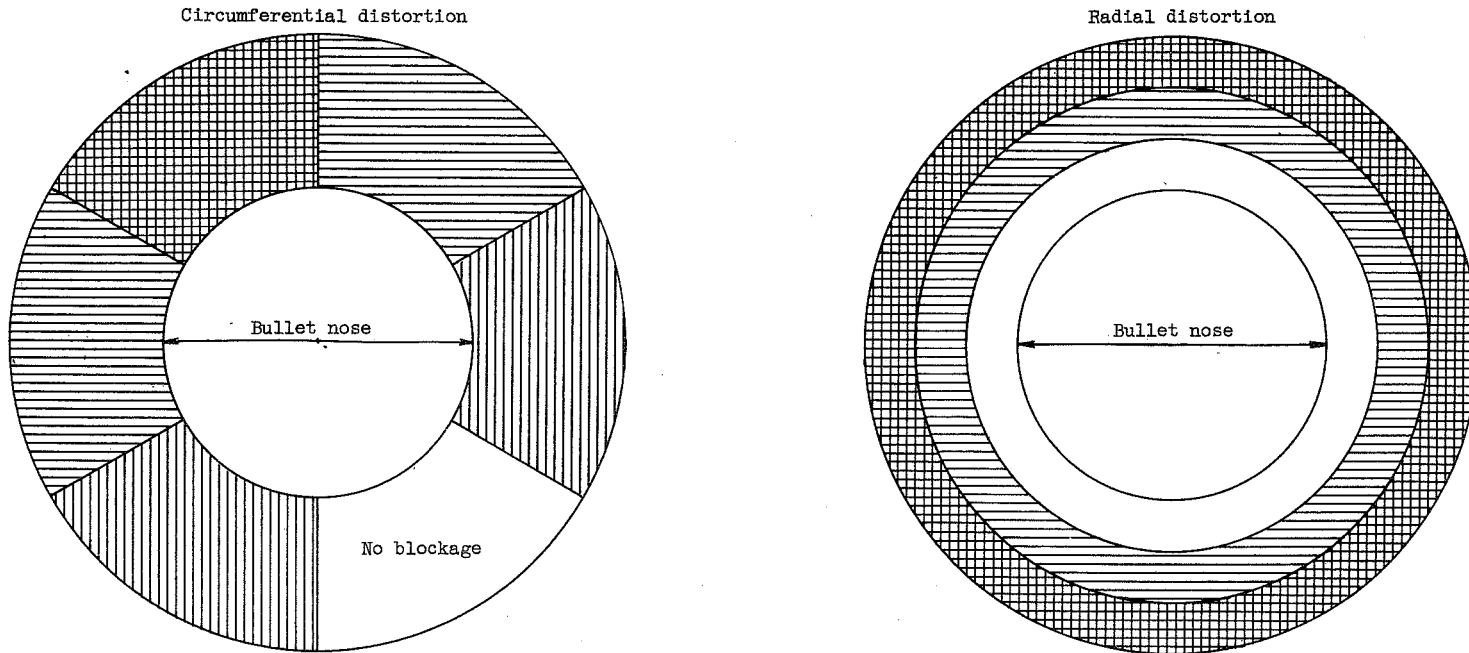
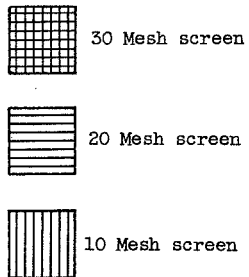


Figure 2. - Location of distortion screens and inlet instrumentation.

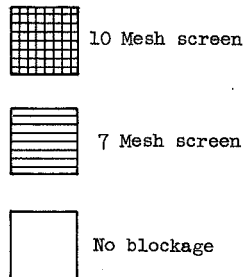


CD-4091

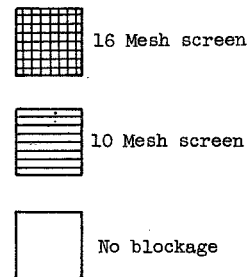
Circumferential "A"



Radial "B"



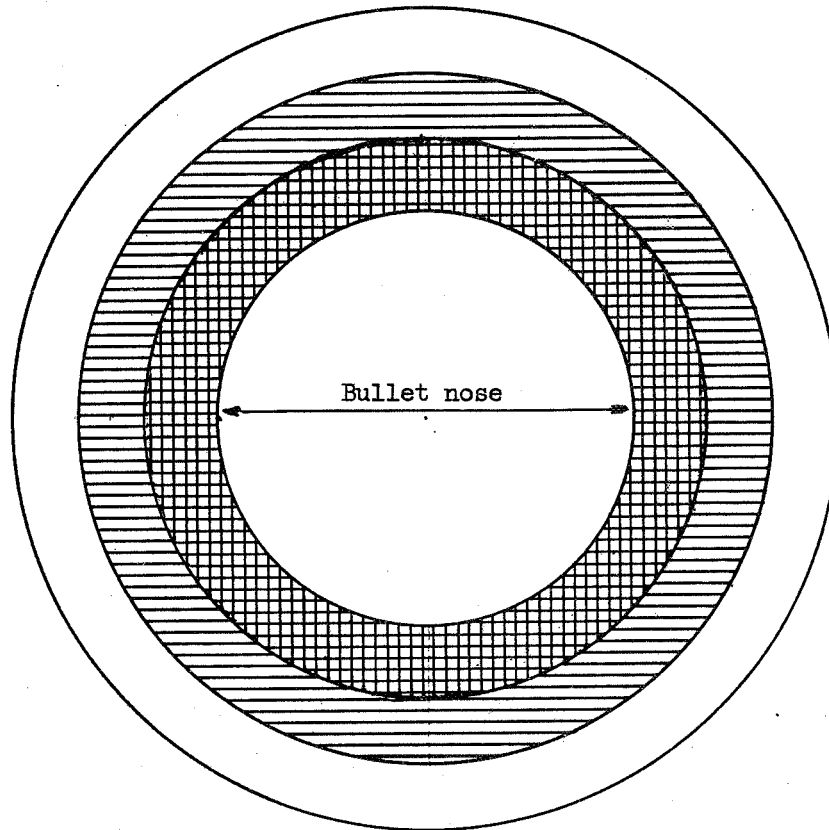
Radial "C"



(Note: Distortion screens were supported on a 1/4" mesh which spanned the inlet annulus).

Figure 3. - Sketch of screen segments for inlet distortion investigation.

## Inverse radial distortion



## Inverse radial "D"



10 Mesh screen



7 Mesh screen



No blockage

CD-4092

(Note: Distortion screens were supported on a 1/4" mesh which spanned the inlet annulus).

Figure 3. - Continued. Sketch of screen segments for inlet distortion investigation.

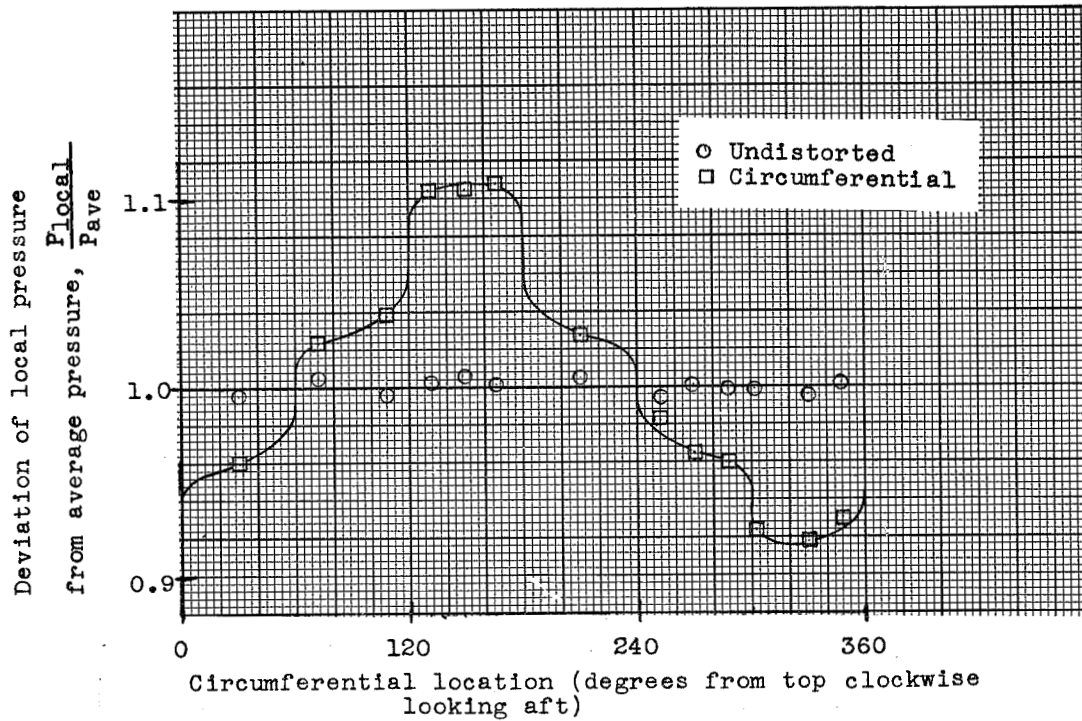


Figure 4(a). Typical circumferential total pressure profile.

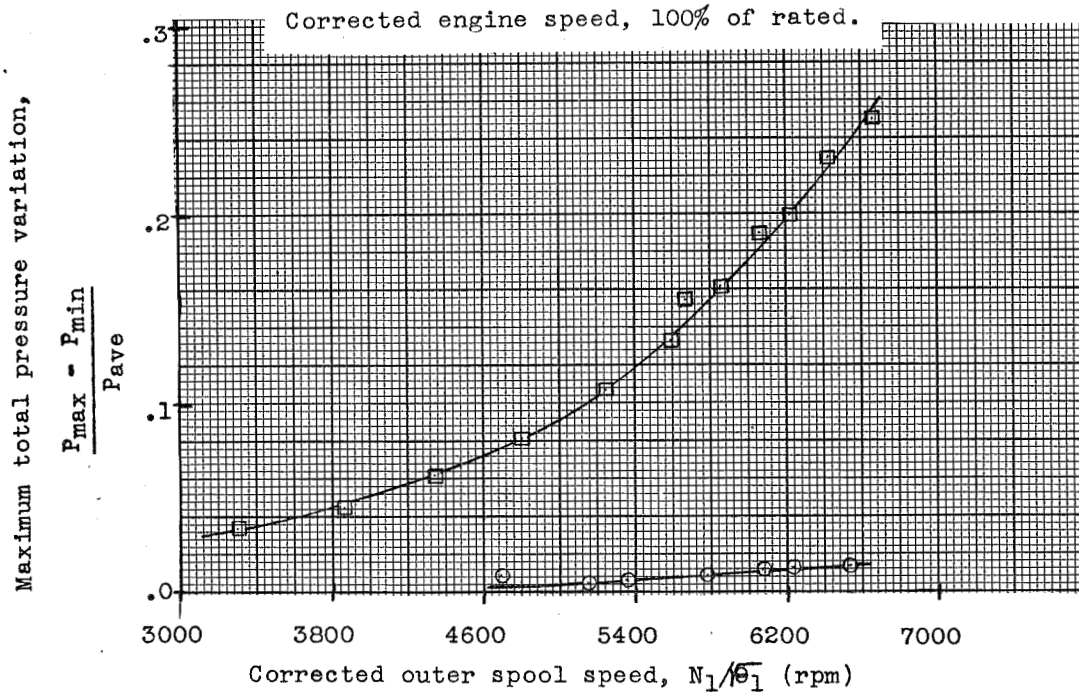


Figure 4(b). Effect of outer compressor corrected speed on the circumferential total pressure gradients. Altitude, 35,000 feet; flight Mach number, 0.8.

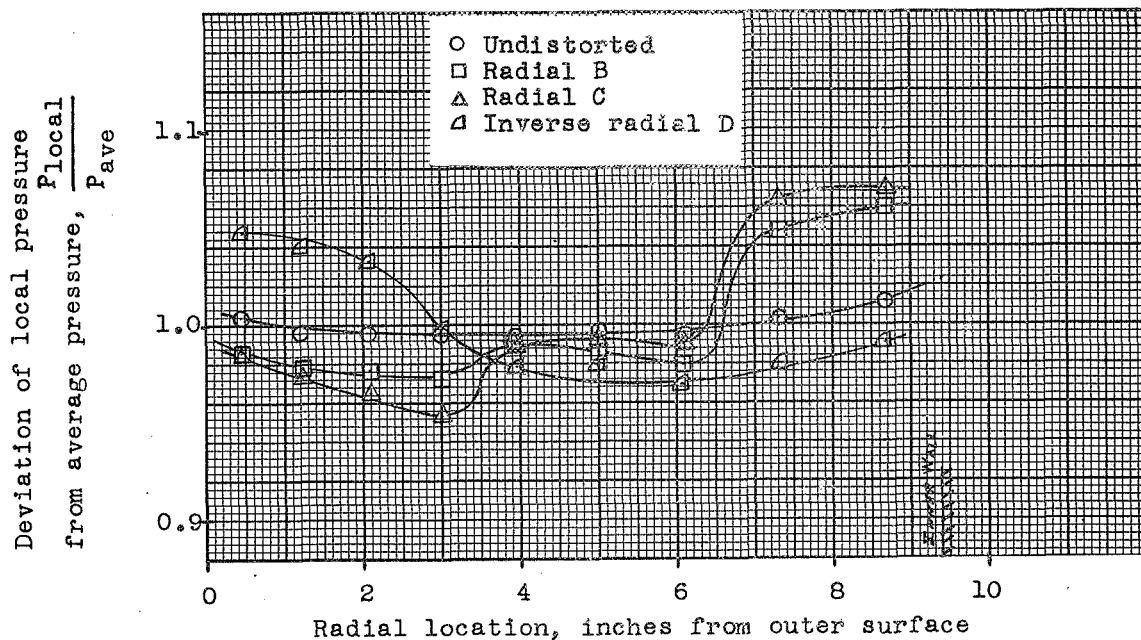


Figure 5(a). Typical radial total pressure profiles.  
 Corrected engine speed, 100% of rated.

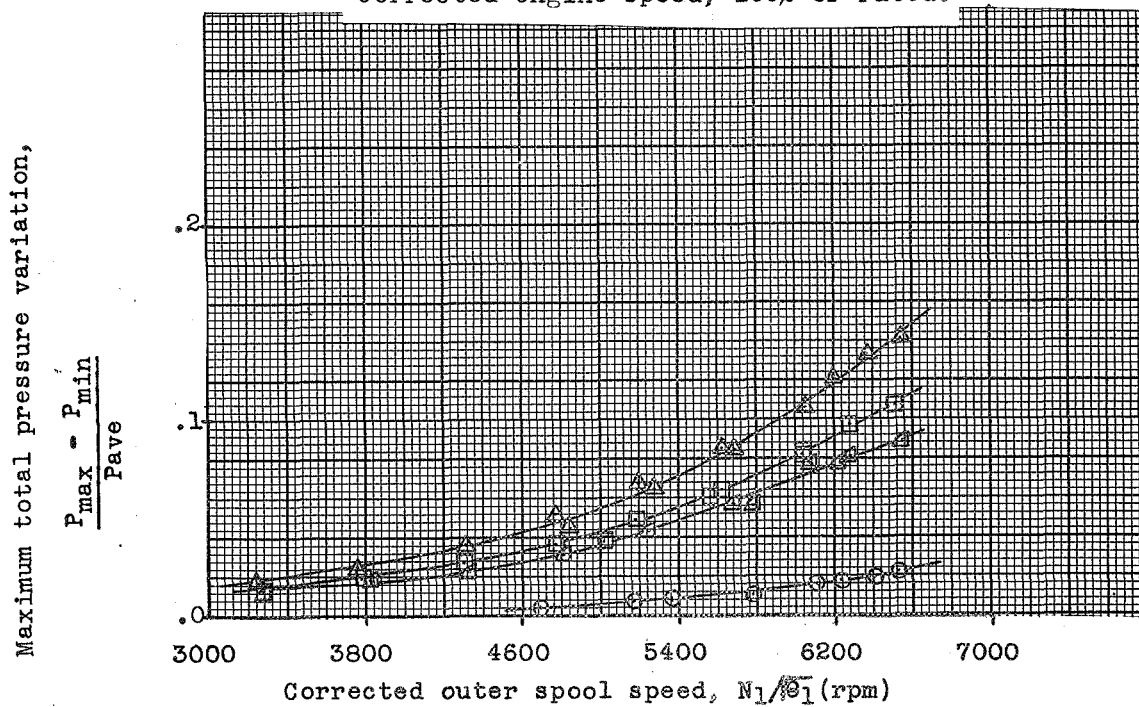


Figure 5(b). Effect of outer compressor corrected speed on the radial total pressure gradients. Altitude, 35,000 feet; flight Mach number, 0.8.

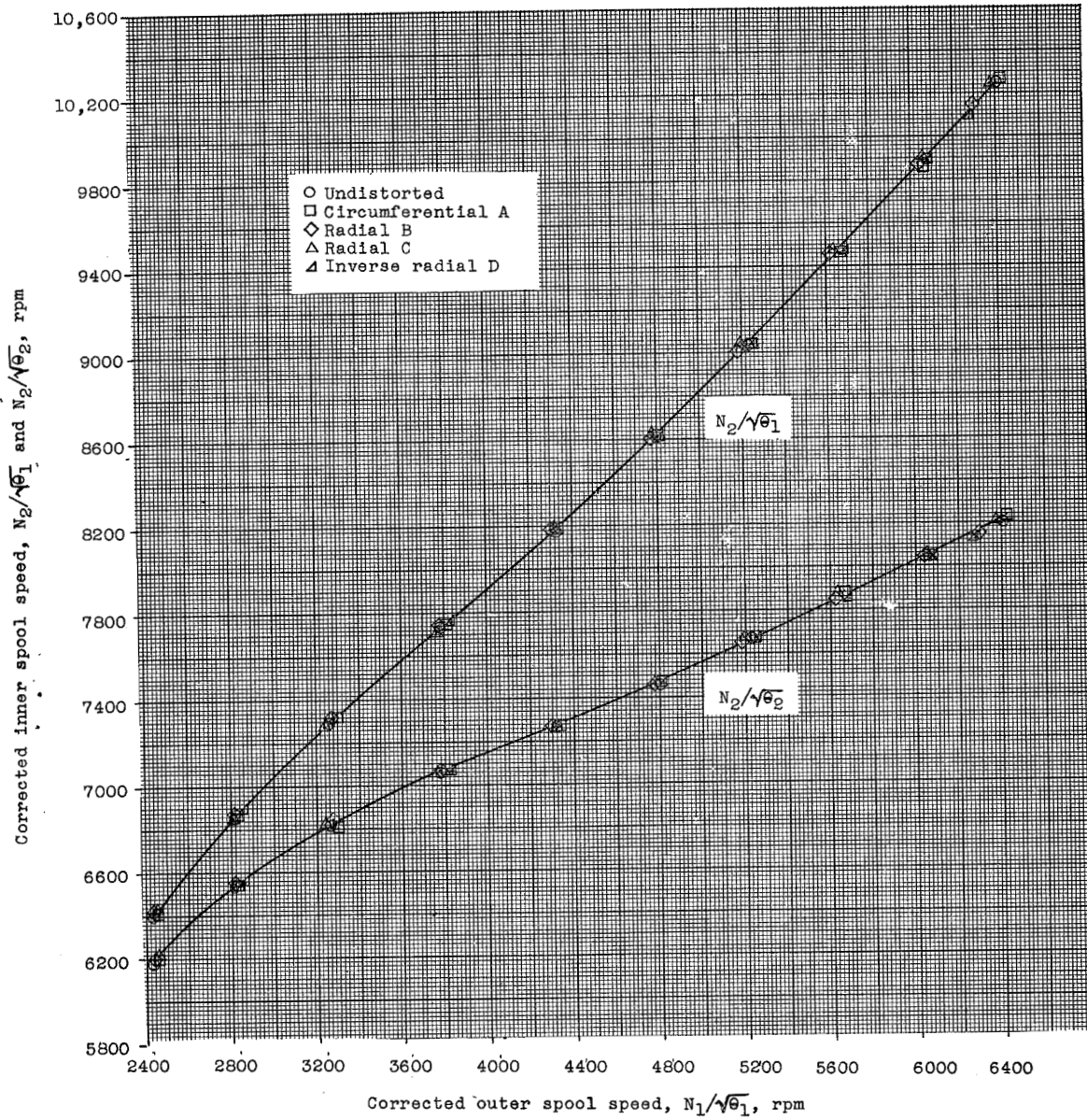


Figure 6. - Variation of corrected inner spool speed with corrected outer spool speed for several inlet pressure distortions. Altitude 35,000 feet, flight Mach number 0.8, compressor bleeds open.

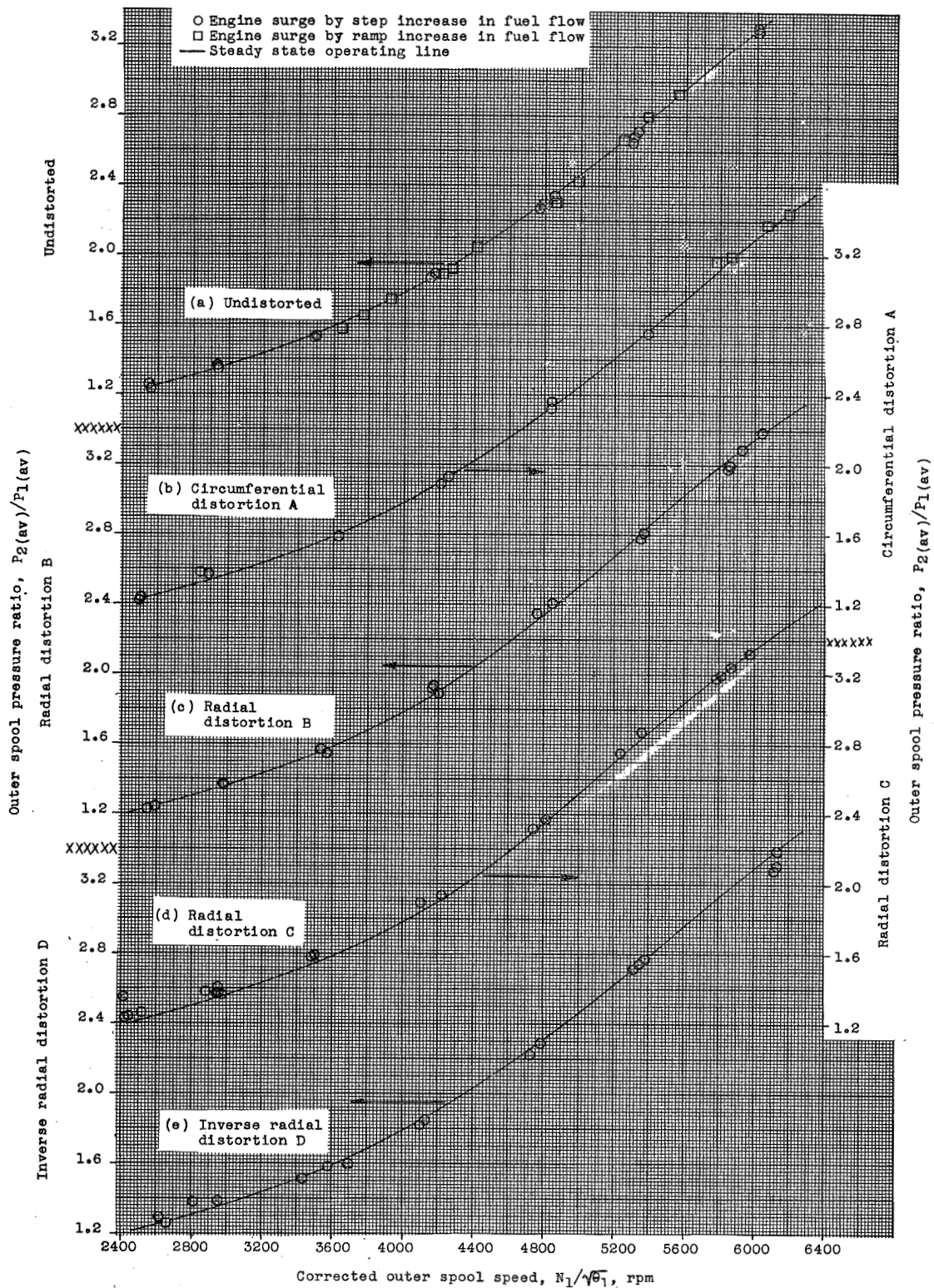


Figure 7. - Comparison of outer spool pressure ratio at engine surge with outer spool steady state operating line for several inlet pressure distortions. Altitude 35,000 feet. Flight Mach number 0.8. Compressor bleeds open.

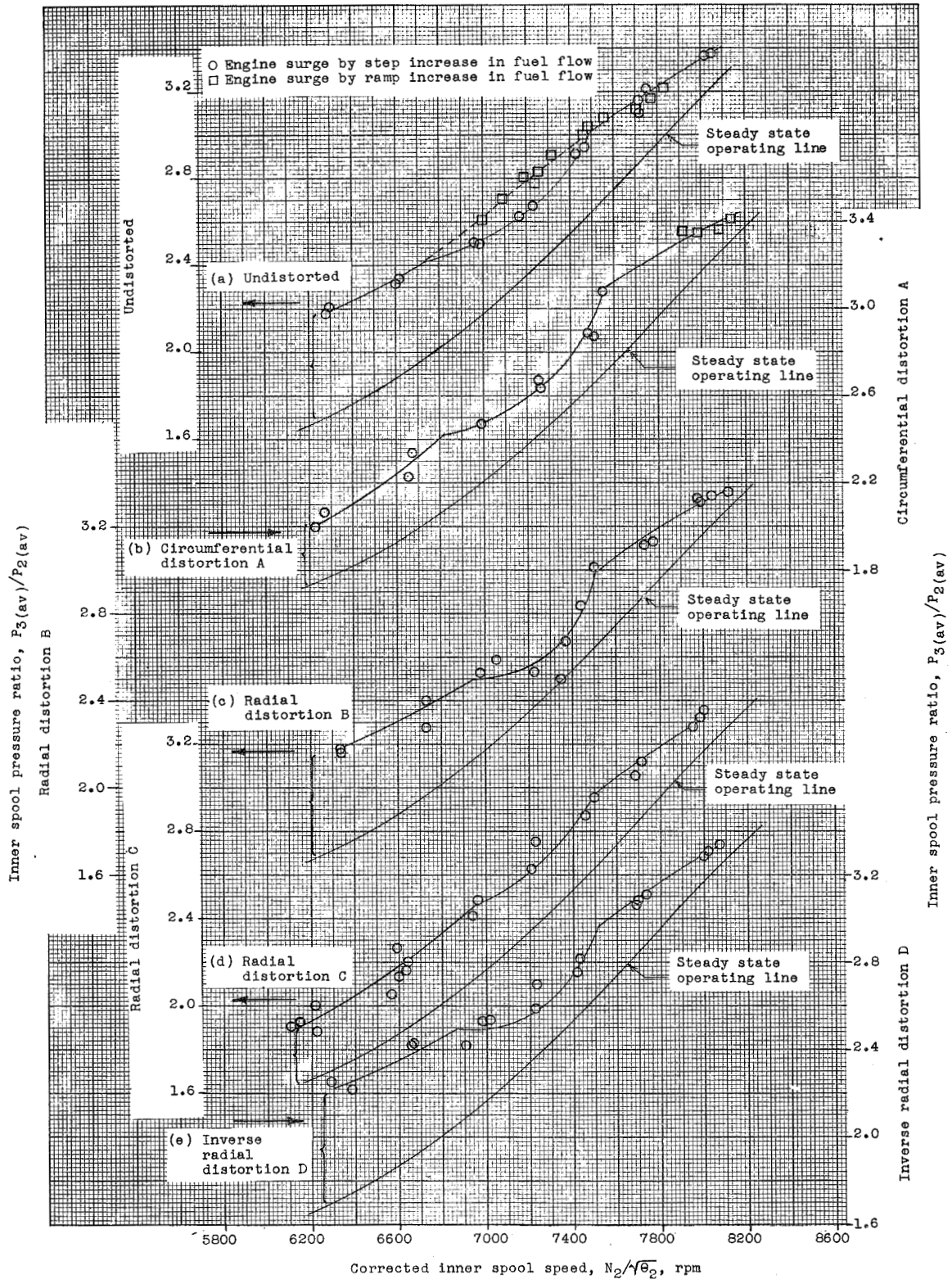


Figure 8. - Comparison of inner spool pressure ratio at engine surge with inner spool steady state operating line for several inlet pressure distortions. Altitude 35,000 feet. Flight Mach number 0.8. Compressor bleeds open.

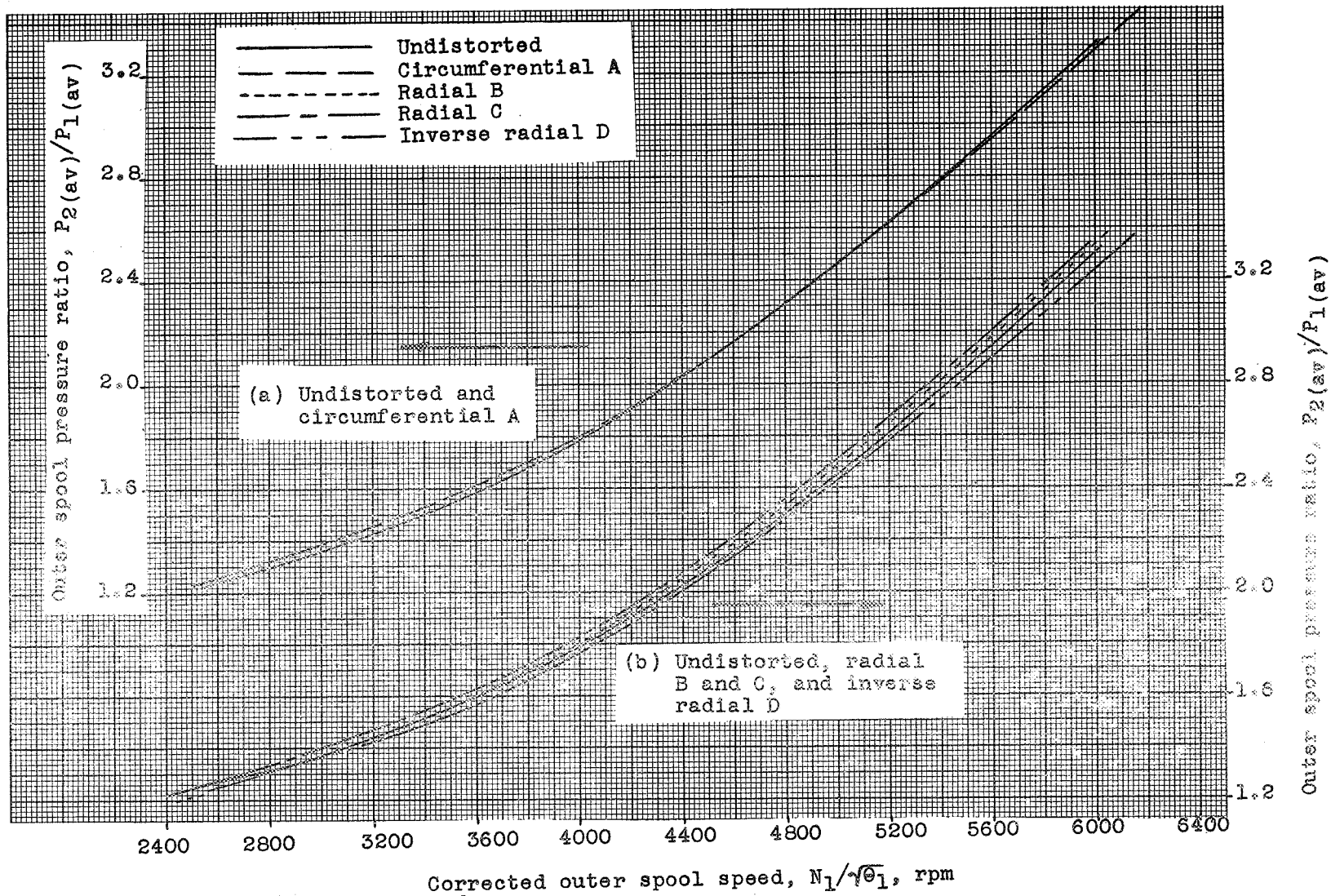


Figure 9. - Effect of inlet pressure distortion on outer spool pressure ratio at engine surge. Altitude 35,000, flight Mach number 0.8, compressor bleeds open.

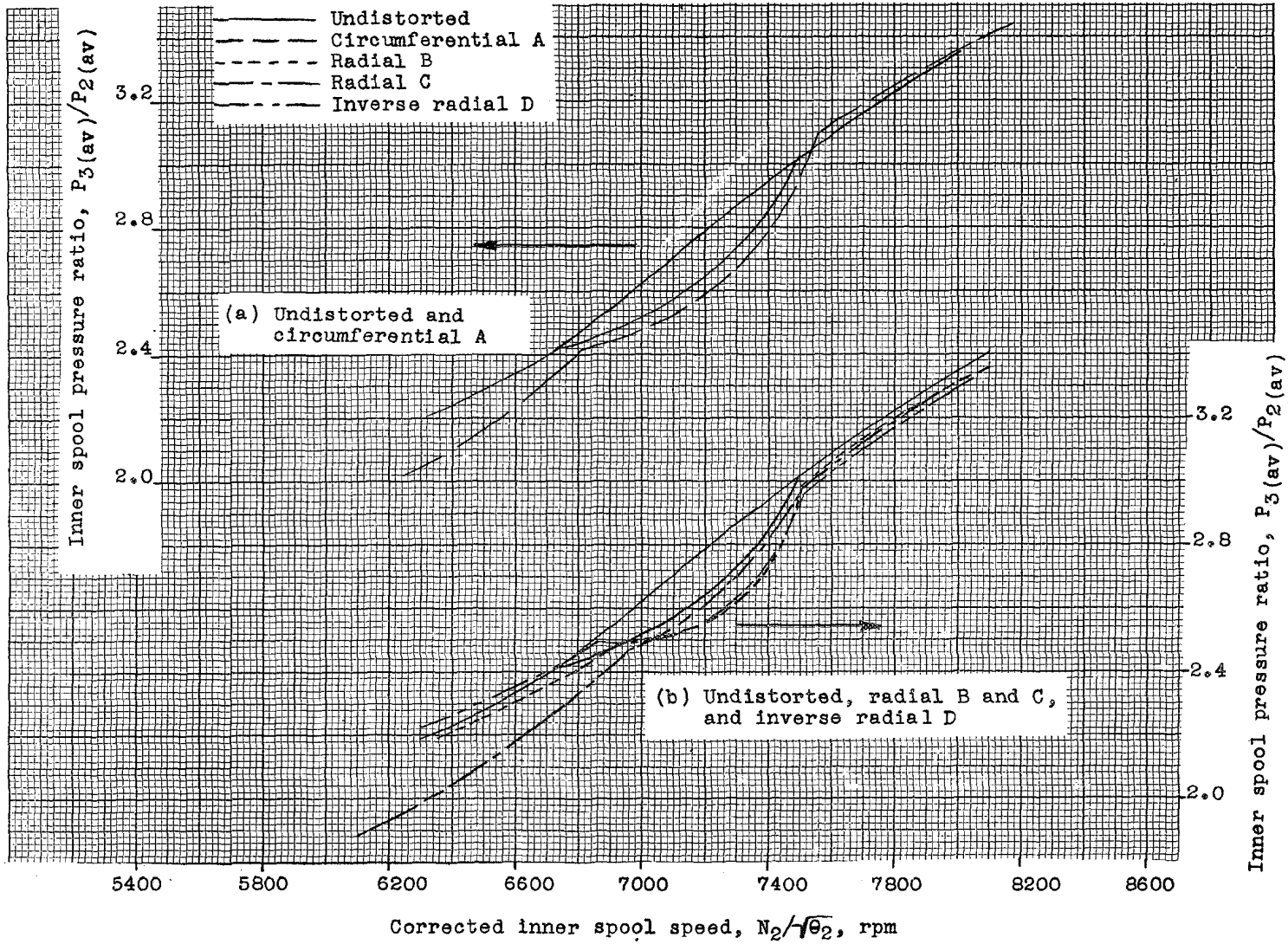


Figure 10. - Effect of inlet pressure distortion on inner spool pressure ratio at engine surge. Altitude 35,000, flight Mach number 0.8, compressor bleeds open.

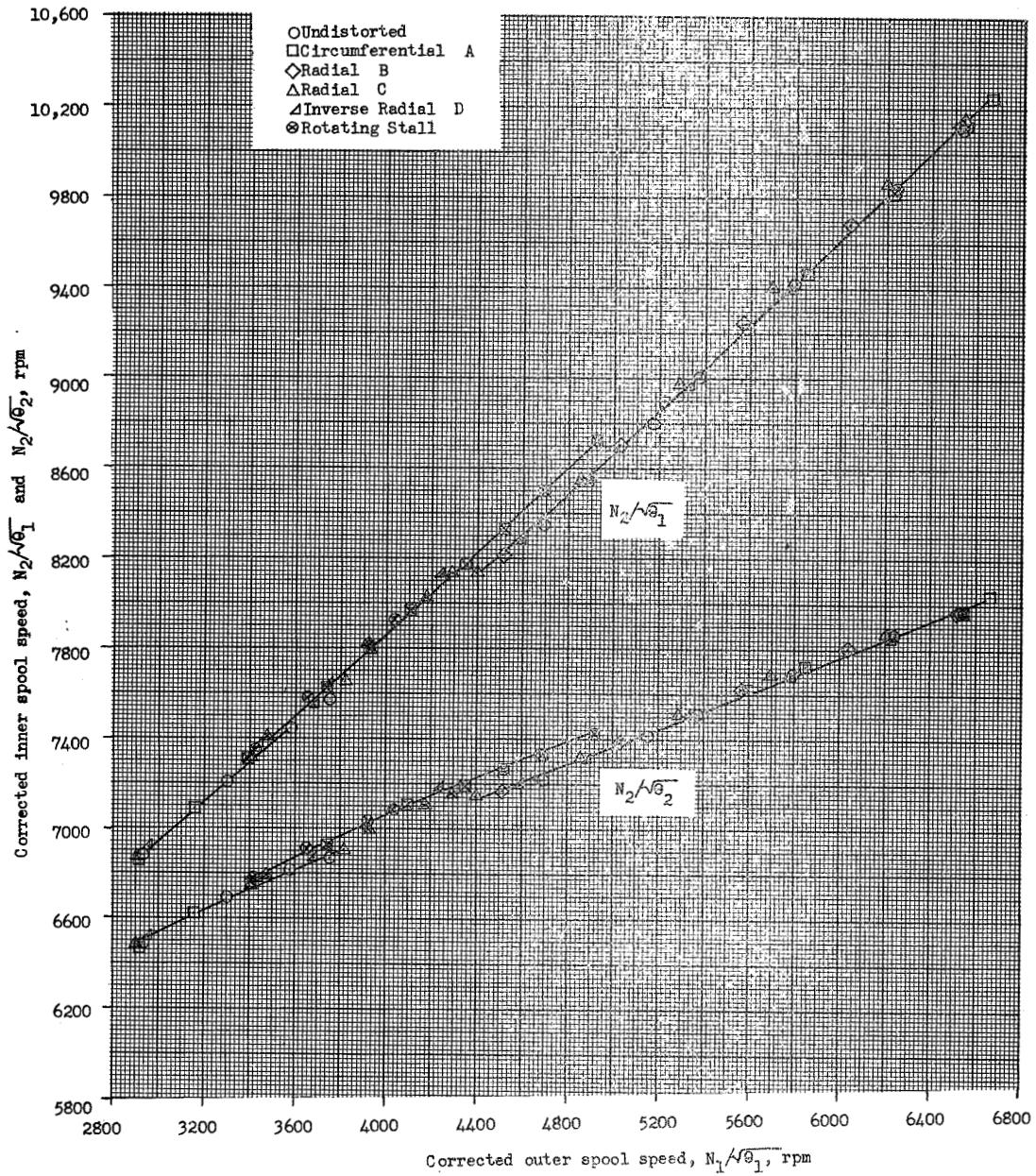


Figure 11. - Variation of corrected inner spool speed with corrected outer spool speed for several inlet pressure distortions. Altitude 35,000 feet. Flight Mach number 0.8. Compressor bleeds closed.

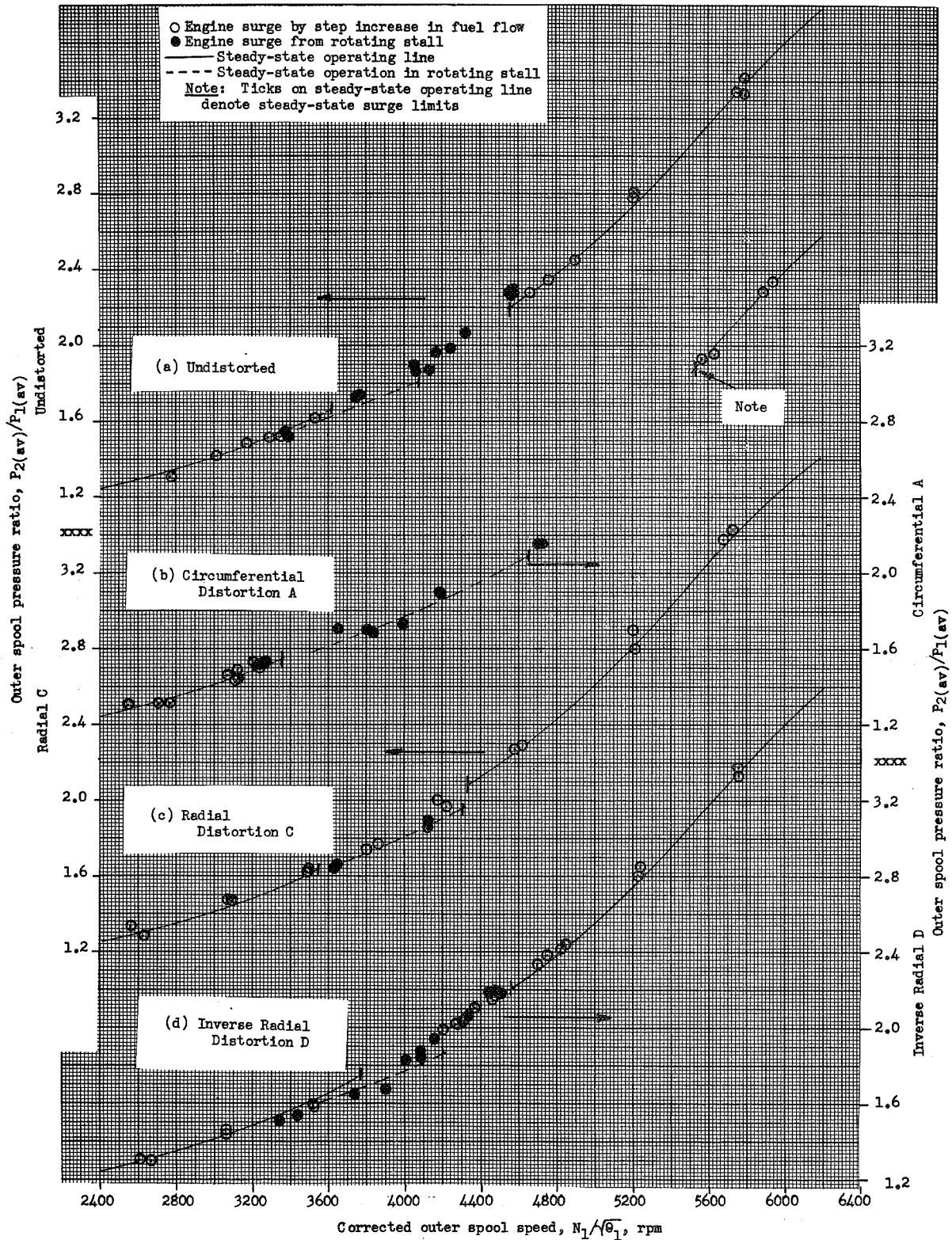


Figure 12. - Comparison of outer spool pressure ratio at engine surge with outer spool steady-state operating line for several inlet pressure distortions. Altitude 35,000 feet. Flight Mach number 0.8. Compressor bleeds closed.

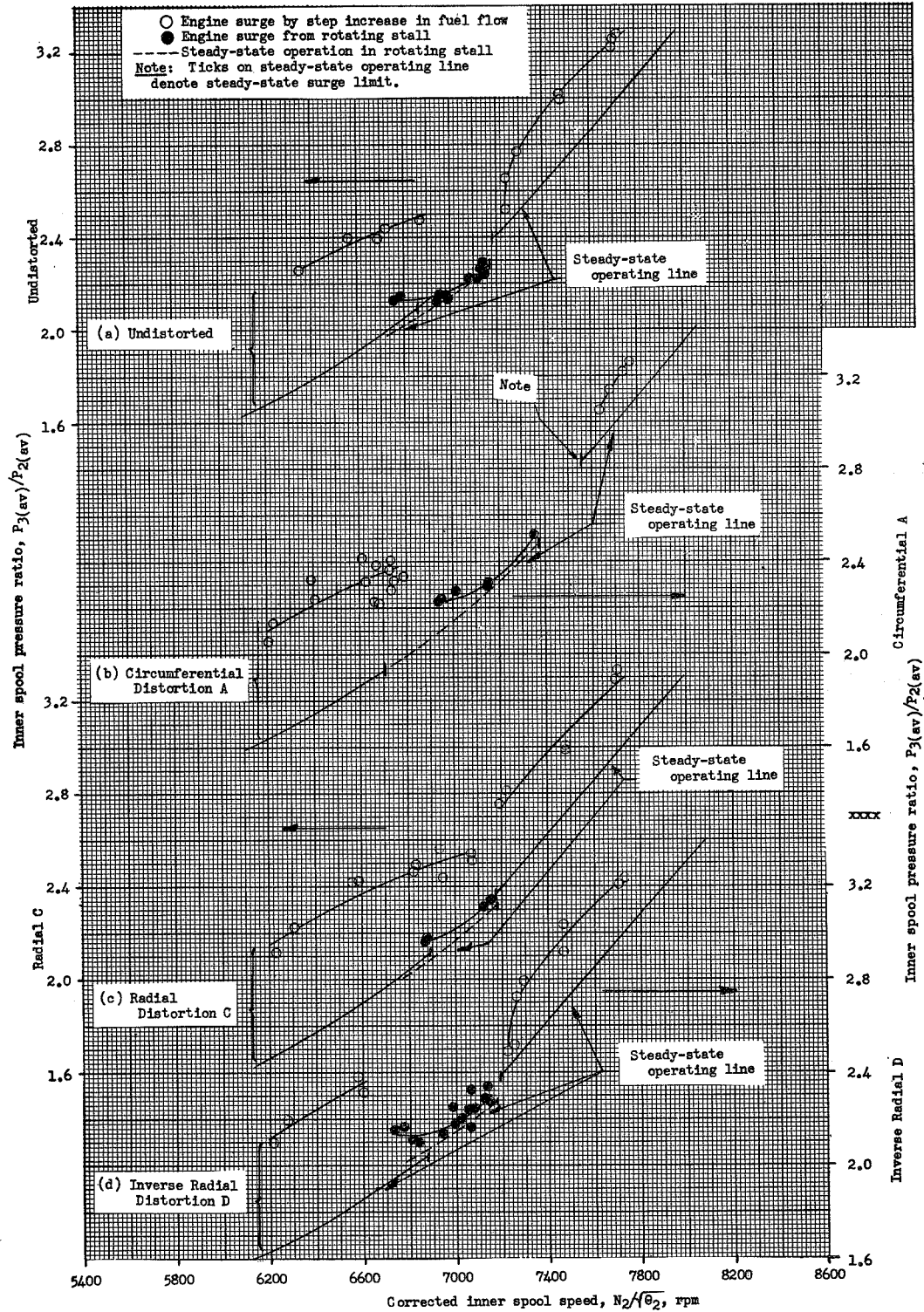


Figure 13. - Comparison of inner spool pressure ratio at engine surge with inner spool steady-state operating line for several inlet pressure distortions. Altitude 35,000 feet. Flight Mach number 0.8. Compressor bleeds closed.

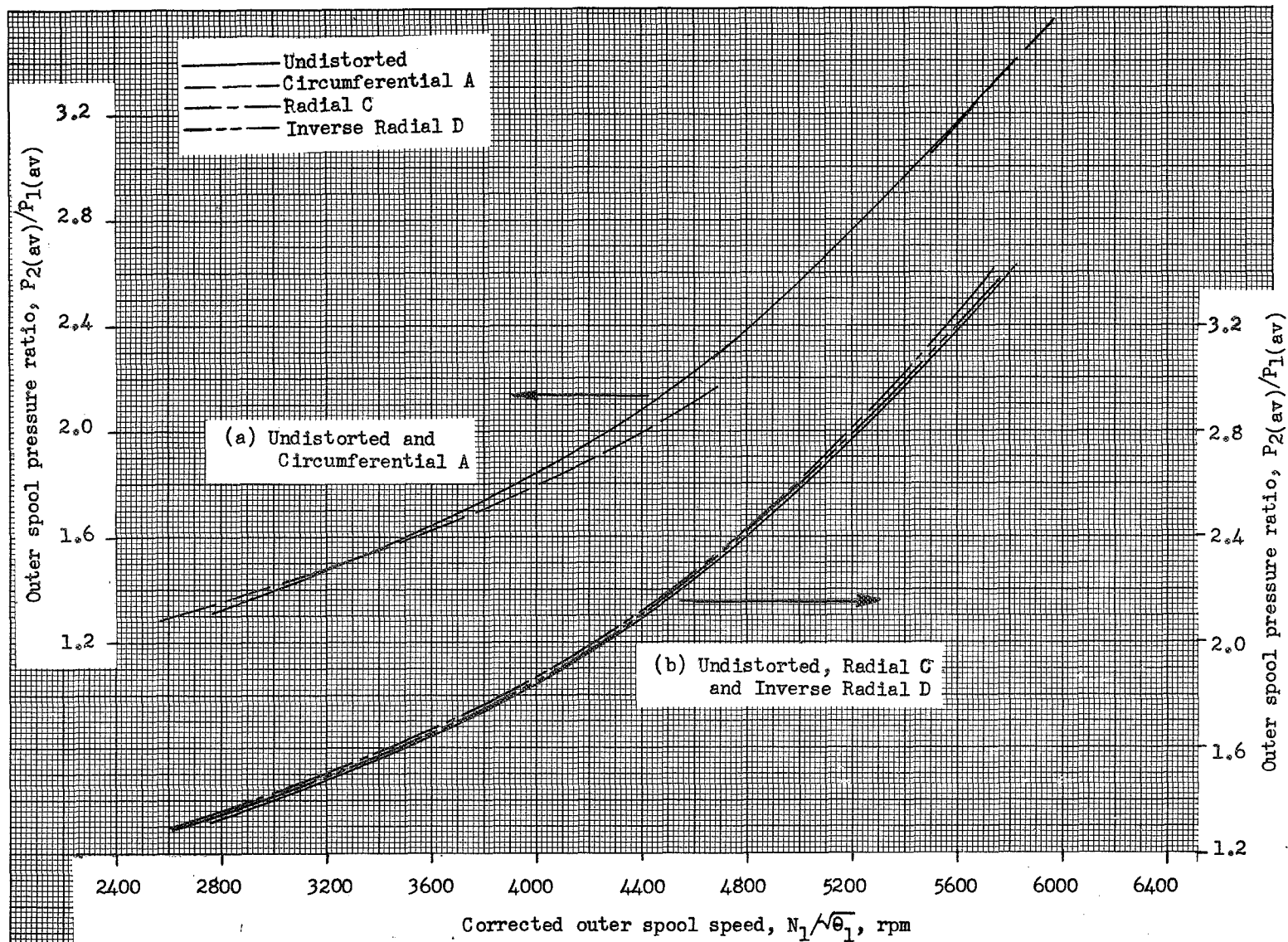


Figure 14. - Effect of inlet pressure distortion on outer spool pressure ratio at engine surge. Altitude 35,000 feet. Flight Mach number 0.8. Compressor bleeds closed.

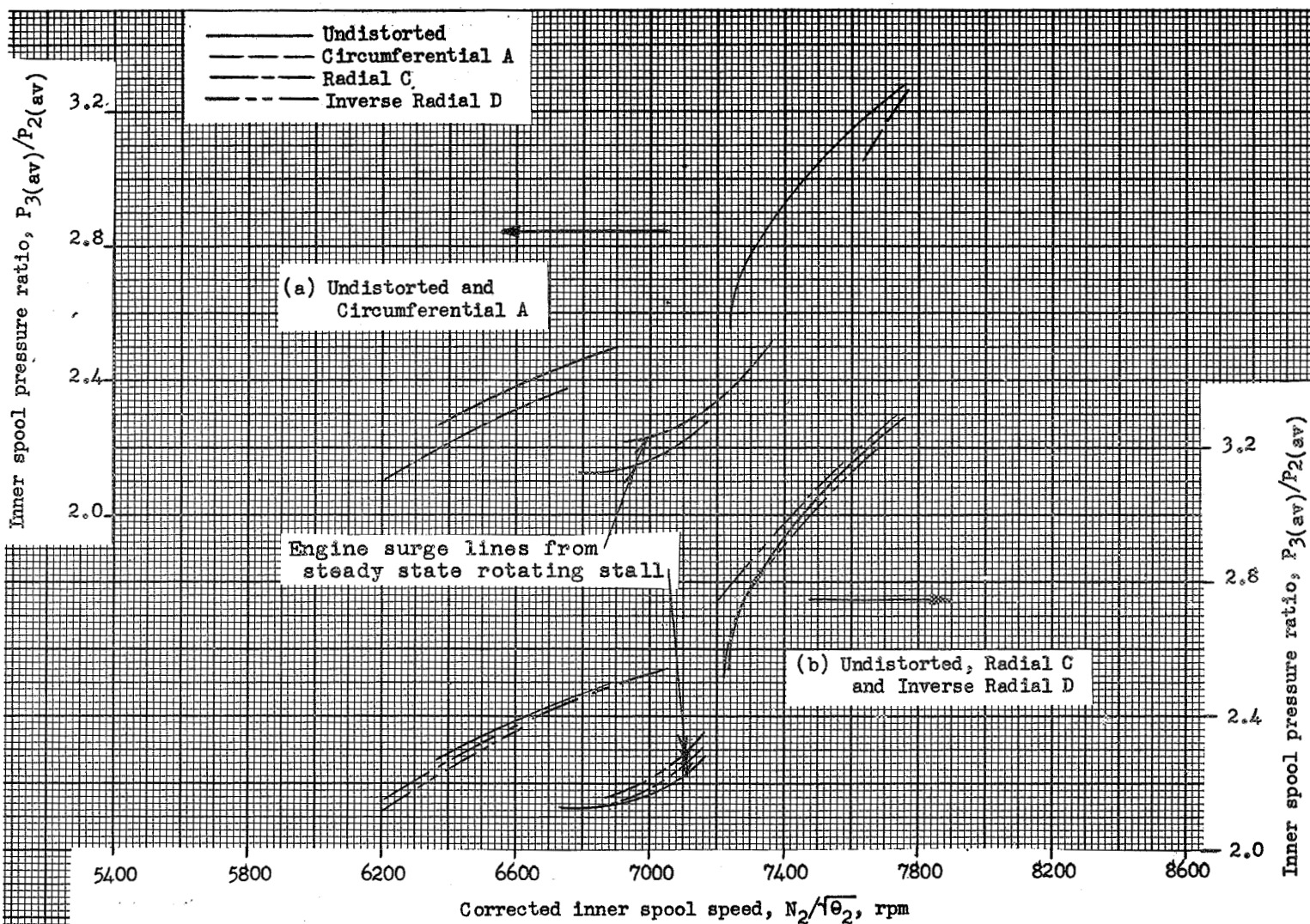


Figure 15. - Effect of inlet pressure distortion on inner spool pressure ratio at engine surge. Altitude 35,000 feet. Flight Mach number 0.8. Compressor bleeds closed.

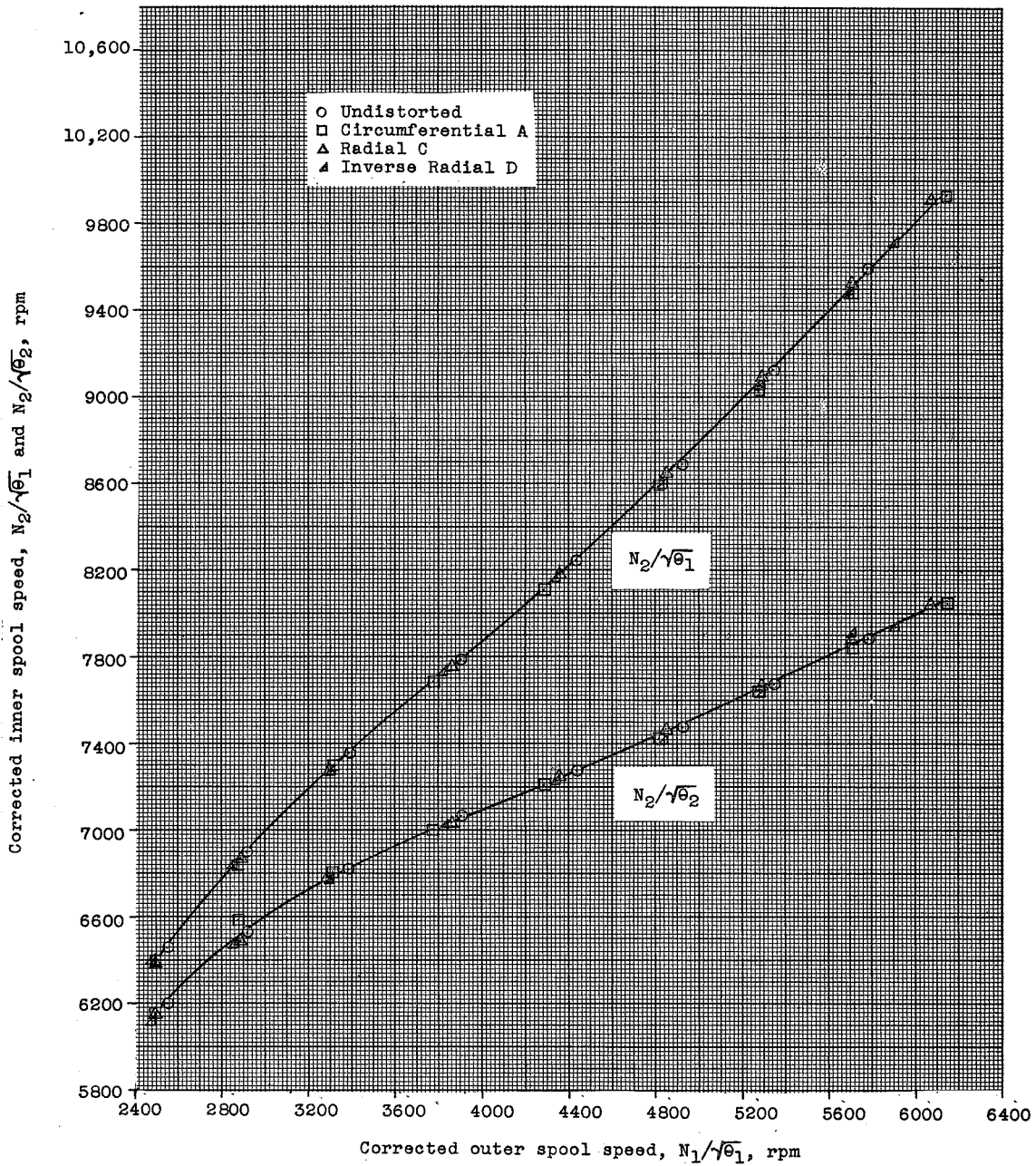


Figure 16. - Variation of corrected inner spool speed with corrected outer spool speed for several inlet pressure distortions. Altitude 50,000, flight Mach number 0.8. Compressor bleeds open.

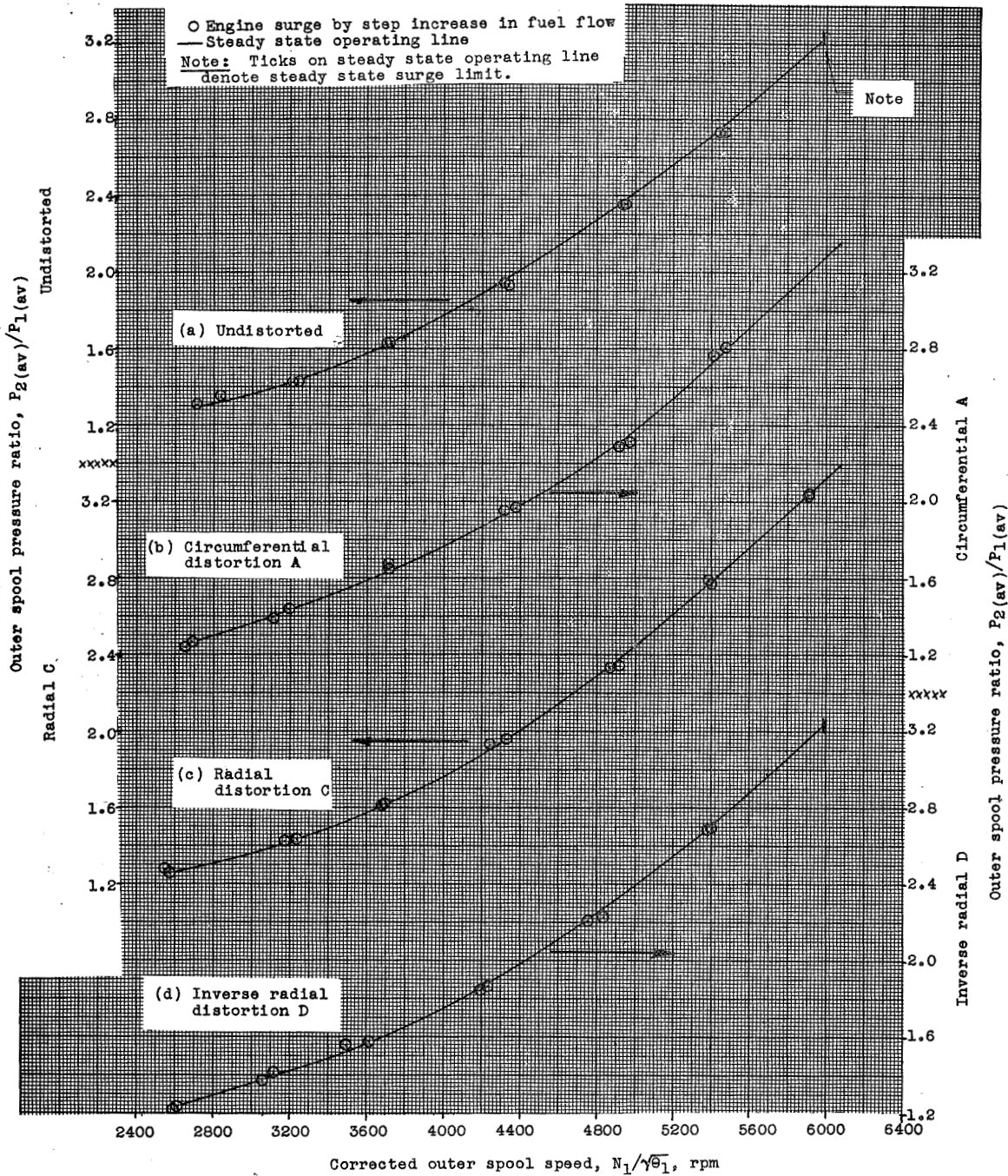


Figure 17. - Comparison of outer spool pressure ratio at engine surge with outer spool steady state operating line for several inlet pressure distortions. Altitude 50,000 feet. Flight Mach number 0.8. Compressor bleeds open.

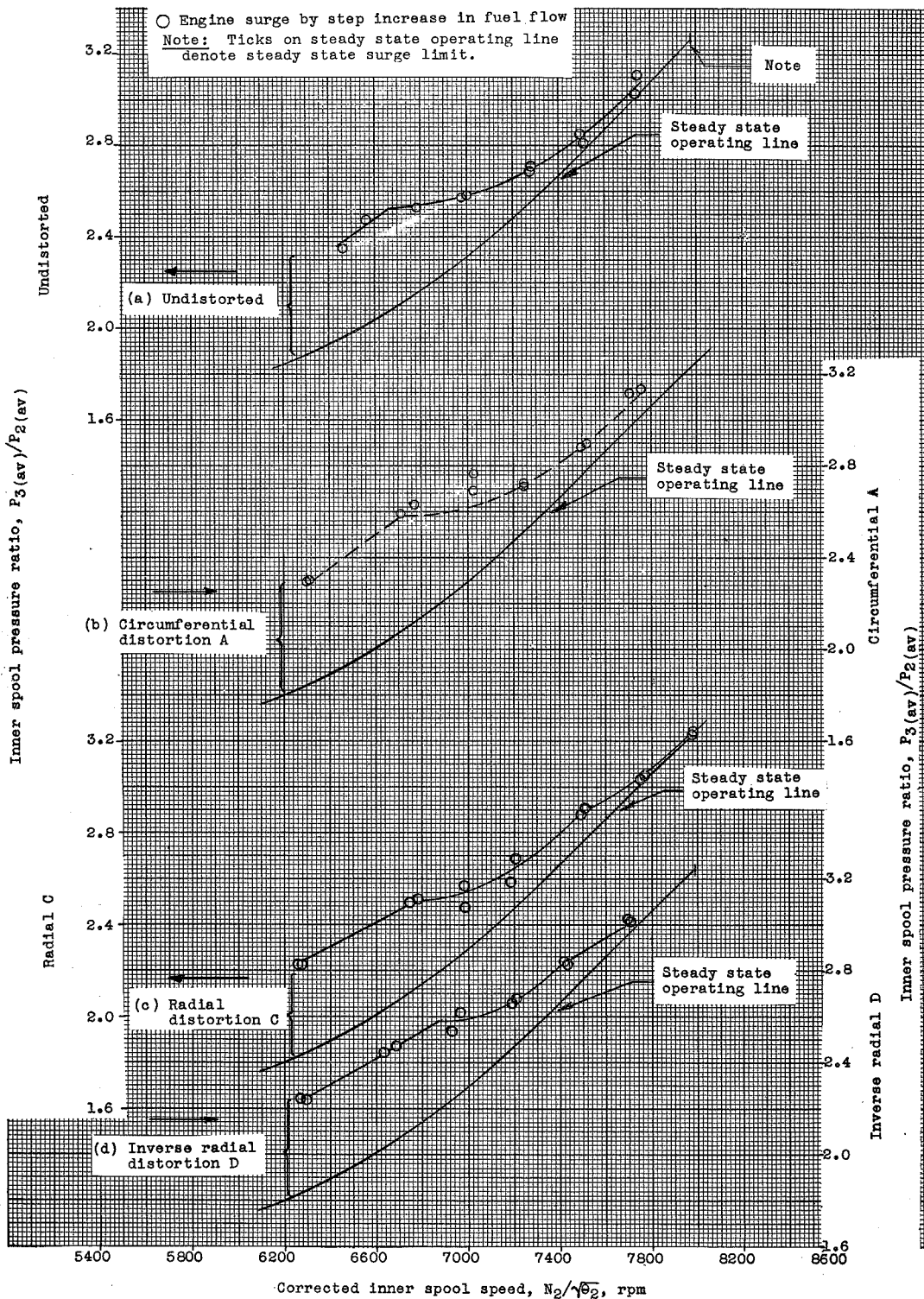


Figure 18. - Comparison of inner spool pressure ratio at engine surge with inner spool steady state operating line for several inlet pressure distortions. Altitude 50,000 feet. Flight Mach number 0.8. Compressor bleeds open.

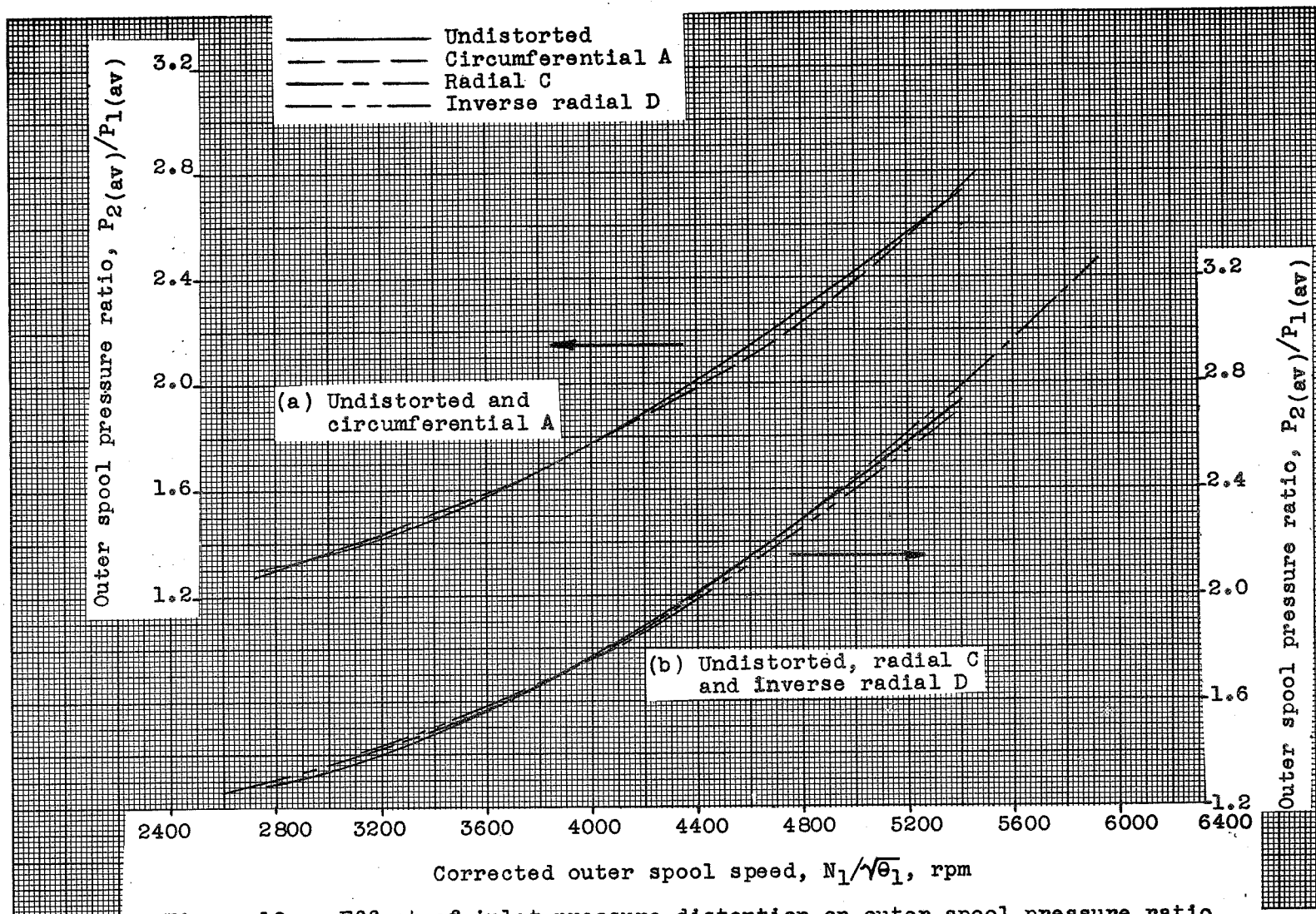


Figure 19. - Effect of inlet pressure distortion on outer spool pressure ratio at engine surge. Altitude 50,000, flight Mach number 0.8, compressor bleeds open.

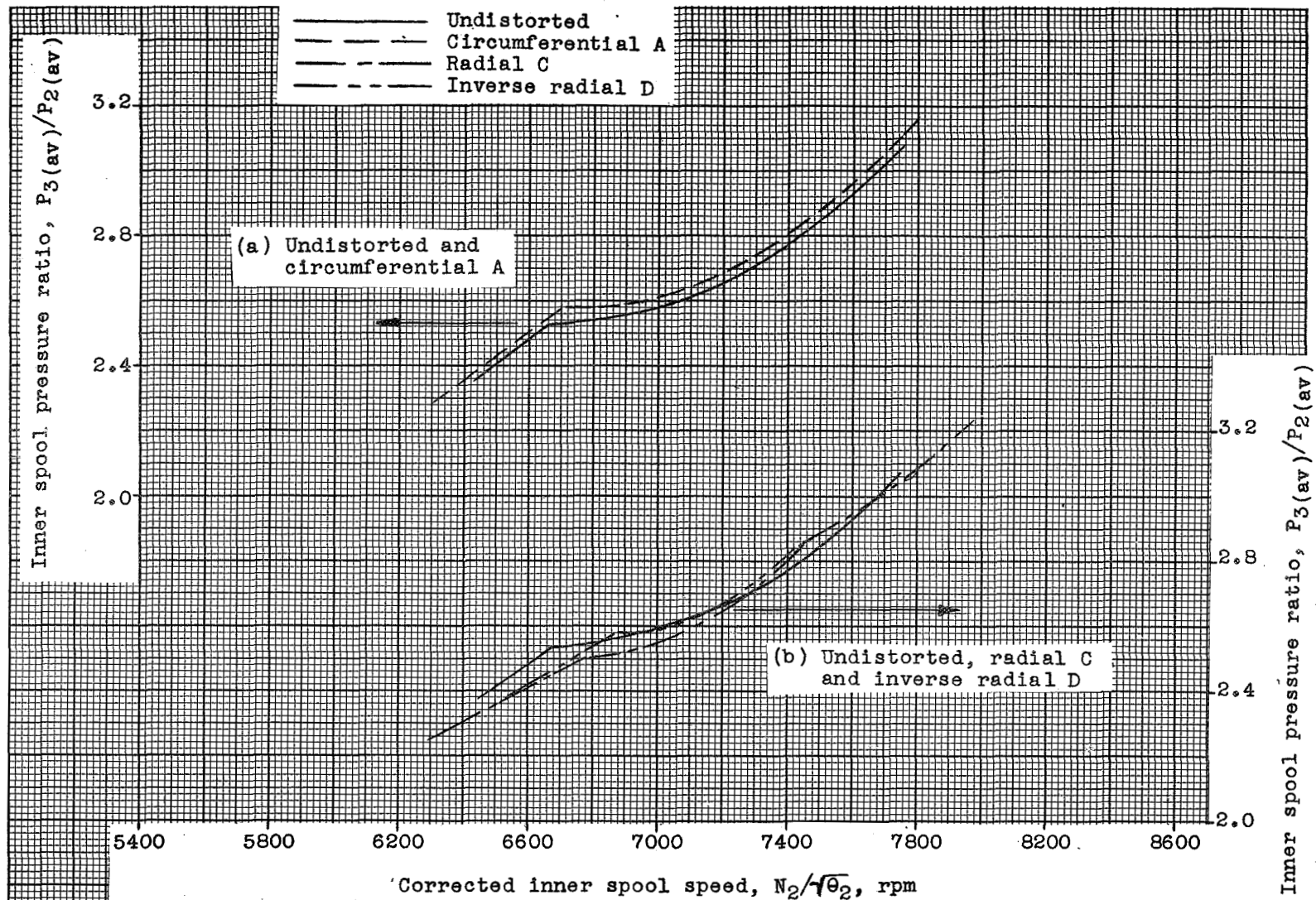


Figure 20. - Effect of inlet pressure distortion on inner spool pressure ratio at engine surge. Altitude 50,000, flight Mach number 0.8, compressor bleeds open.

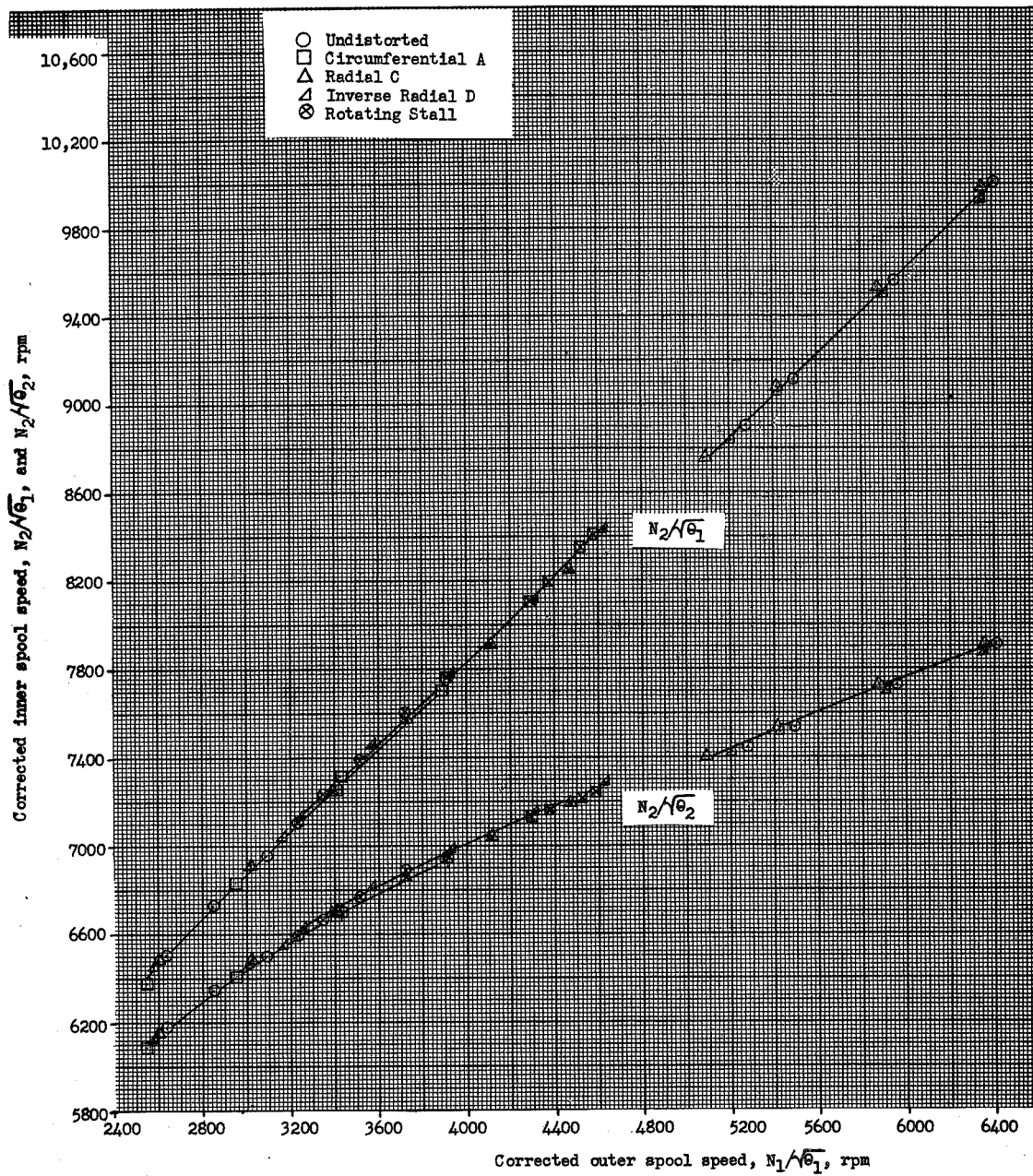


Figure 21. - Variation of corrected inner spool speed with corrected outer spool speed for several inlet pressure distortions. Altitude 50,000 feet. Flight Mach number 0.8. Compressor bleeds closed.

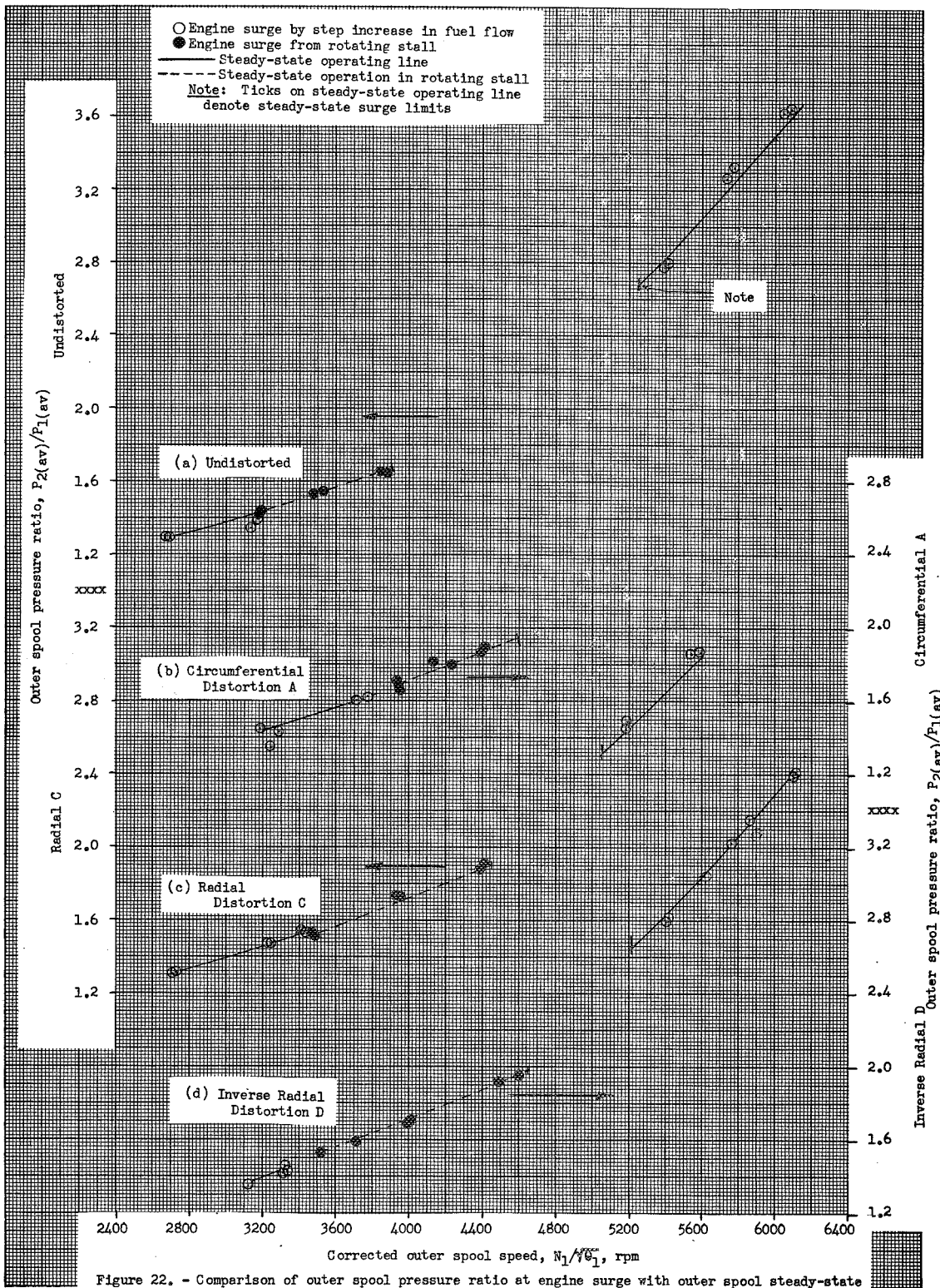


Figure 22. - Comparison of outer spool pressure ratio at engine surge with outer spool steady-state operating line for several inlet pressure distortions. Altitude 50,000 feet. Flight Mach number 0.8. Compressor bleeds closed.

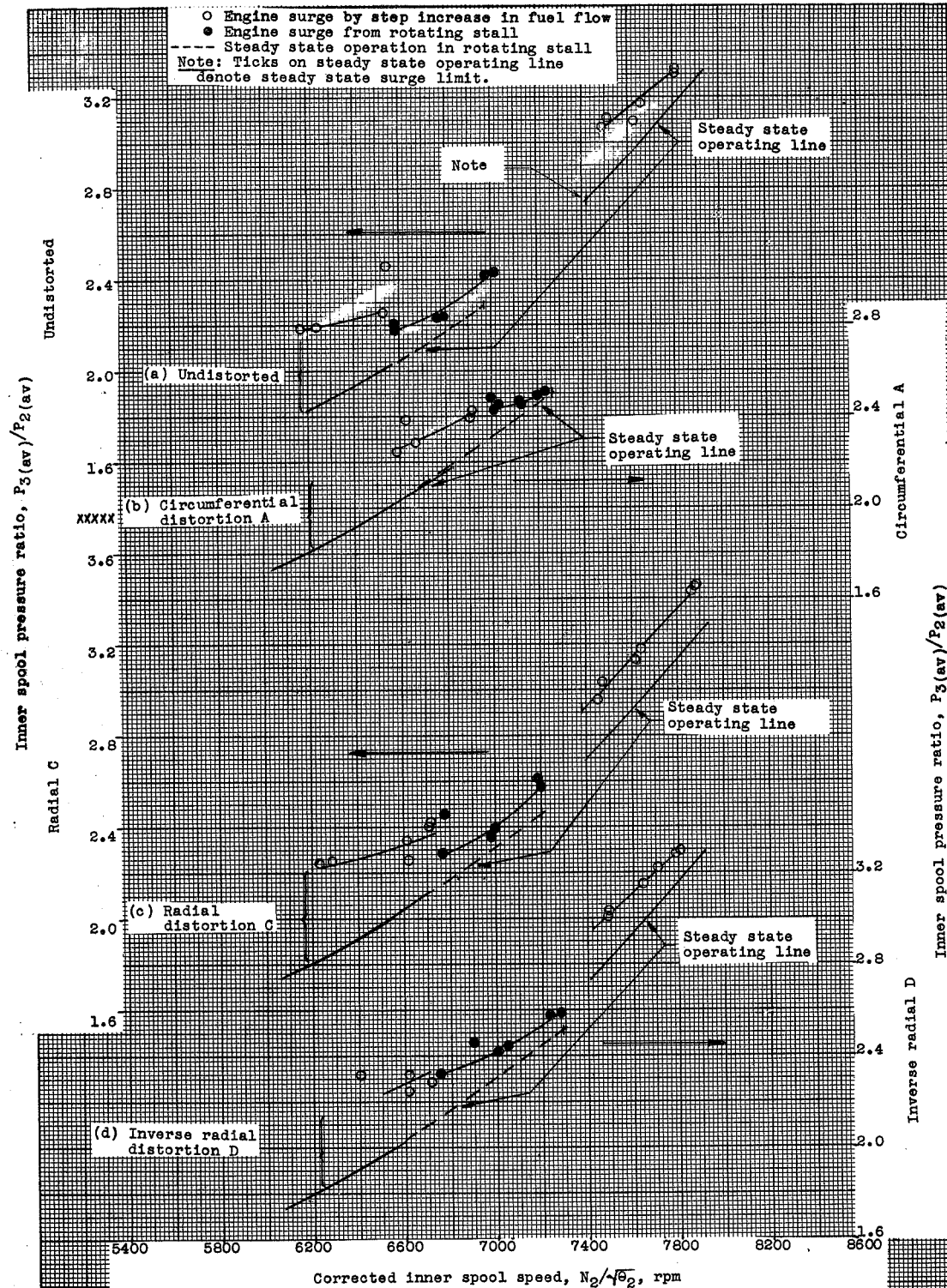


Figure 23. - Comparison of inner spool pressure ratio at engine surge with inner spool steady state operating line for several inlet pressure distortions. Altitude 50,000 feet. Flight Mach number 0.8. Compressor bleeds closed.

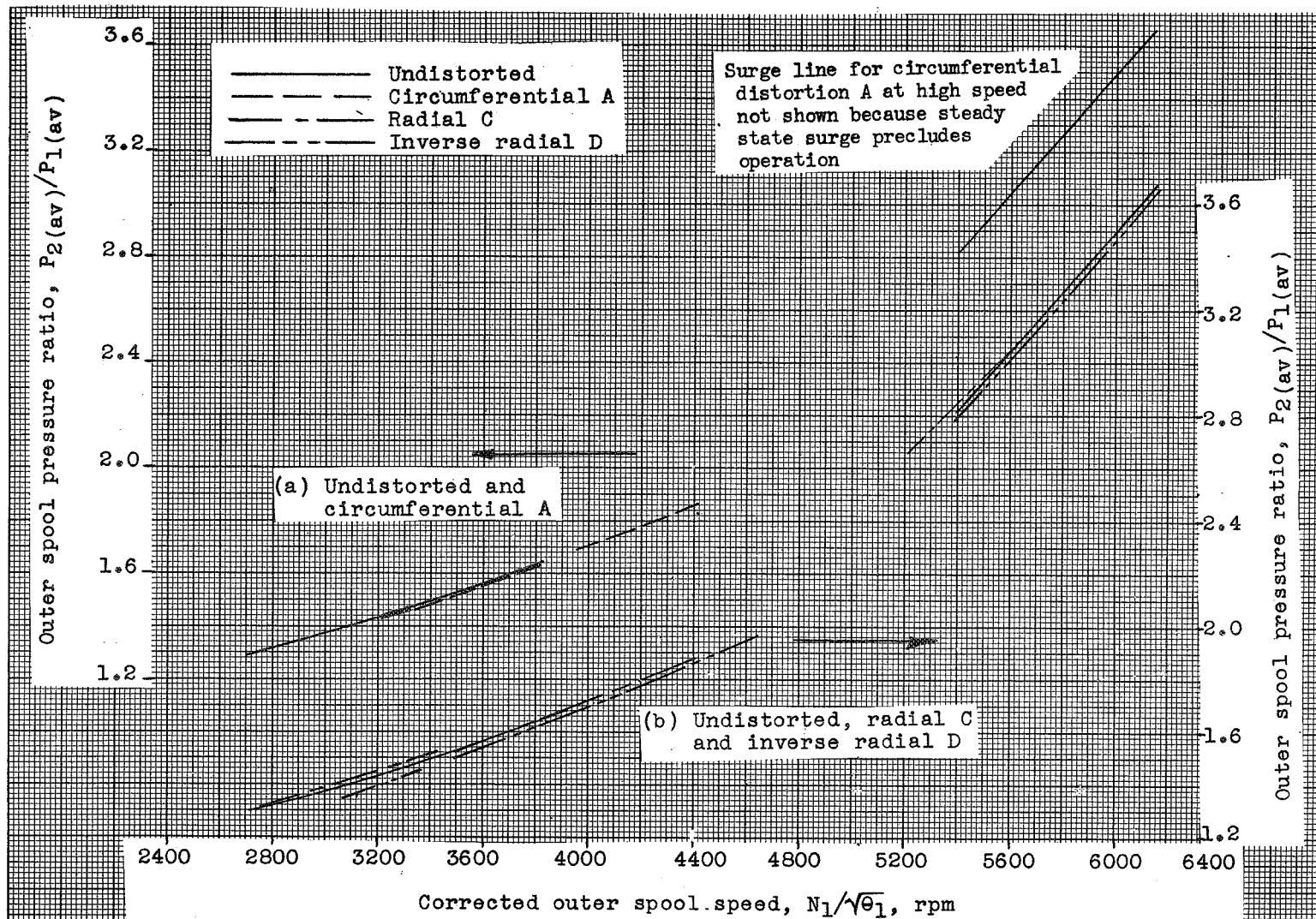


Figure 24. - Effect of inlet pressure distortion on outer spool pressure ratio at engine surge. Altitude 50,000, flight Mach number 0.8, compressor bleeds closed.

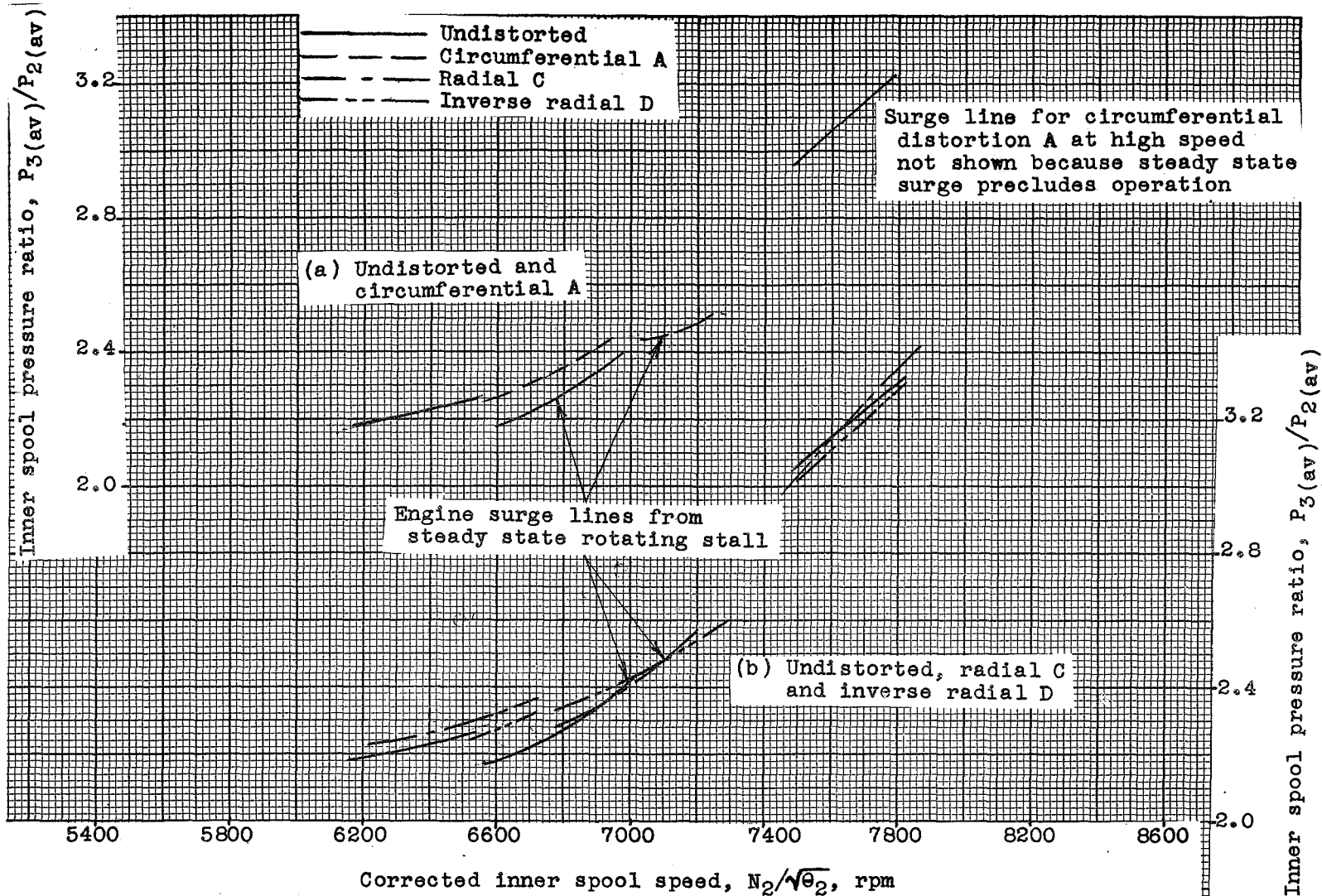


Figure 25. - Effect of inlet pressure distortion on inner spool pressure ratio at engine surge. Altitude 50,000, flight Mach number 0.8, compressor bleeds closed.

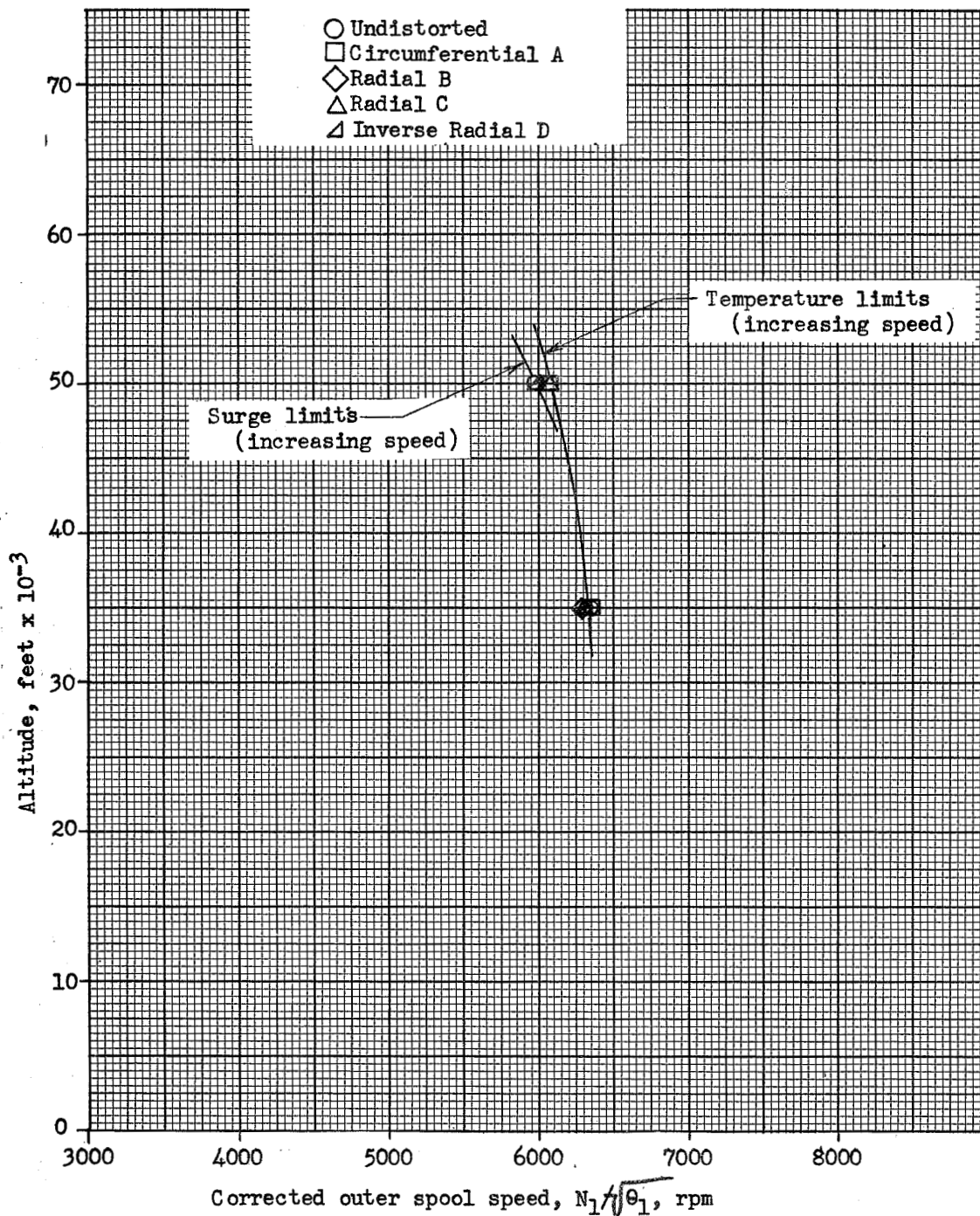


Figure 26. - Effect of altitude on engine operating limits.  
 Flight Mach number 0.8. Compressor bleeds open.

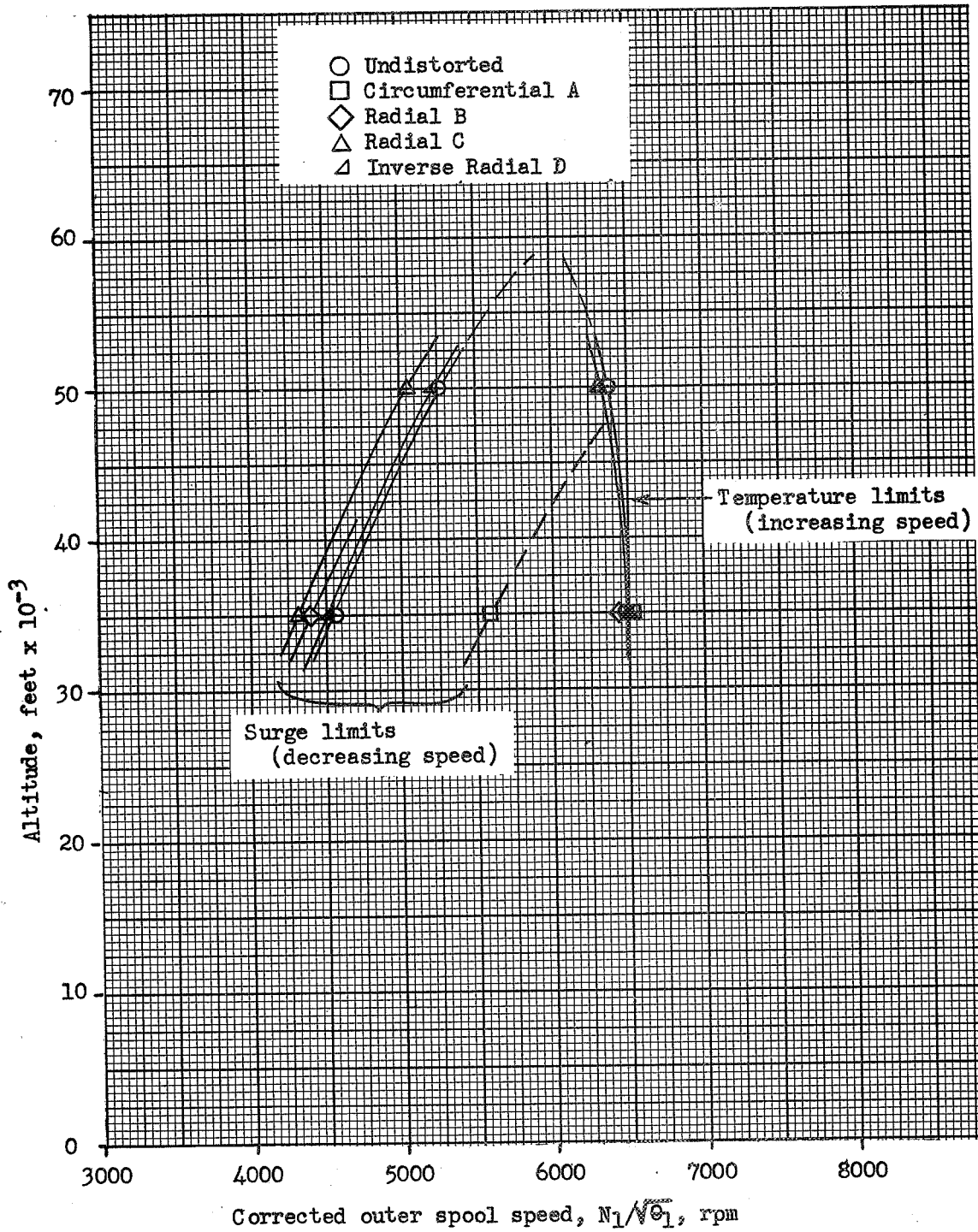


Figure 27. - Effect of altitude on engine operating limits.  
Flight Mach number 0.8. Compressor bleeds closed.

3599

PRELIMINARY DATA ON THE EFFECTS OF INLET PRESSURE DISTORTIONS

ON THE J57-P-1 TURBOJET ENGINE



Lewis E. Wallner  
Aeronautical Research Scientist  
Propulsion Systems



Robert J. Lubick  
Aeronautical Research Scientist  
Propulsion Systems



Thomas H. Einstein  
Aeronautical Research Intern  
Aerodynamics

Approved:



William A. Fleming  
Aeronautical Research Scientist  
Propulsion Systems



Bruce T. Lundin  
Chief  
Engine Research Division

cak - 12/3/54